ELECTROSPUN BIODEGRADABLE POLYMERIC MEMBRANES FOR POST-SURGERY ANTI-ADHESION APPLICATIONS

by

POURISKA BIGVAND KIVANANY

Presented to the Faculty of the Graduate School of

The University of Texas at Arlington in Partial Fulfillment

of the Requirements

for the Degree of

MASTER OF SCIENCE IN BIOENGINEERING

THE UNIVERSITY OF TEXAS AT ARLINGTON

FALL 2012

ACKNOWLEDGEMENTS

I would like to thank Dr. Jian Yang for allowing me an opportunity to work in his lab, providing me with direction in my research, and exposing me to the incredible field of biomaterials. I am grateful to Dr. Kytai T. Nguyen for kindly allowing me to work in her lab to complete this project and for helping me to become a better researcher. I would also like to thank my committee members, Dr. Baohong Yuan and Dr. Yi Hong, for taking time to serve on my committee.

I would like to express my gratitude to Dr. Zhiwei Xie for guiding me throughout this study and teaching me life-long research skills that I shall carry with me into future. Without his patience, support, and training, I would not have been able to complete this project.

I would also like to express my appreciation to my dear friend Anna, and my sister, Sanam. Your uplifting words and positive energy have been inspiring. My utmost gratefulness to my love, Marco, for being selfless, supportive, and motivating.

Most importantly, I would like to thank my Father, Reza, for not only financially supporting me during my academic career, but also for emotionally supporting me through all walks of life. I could not have completed my project without your encouraging words or the stress-free home you have provided for me. This thesis is especially dedicated to my Father.

November 14, 2012

ABSTRACT

ELECTROSPUN BIODEGRADABLE POLYMERIC

MEMBRANES FOR POST-SURGERY

ANTI-ADHESION APPLICATIONS

Pouriska Kivanany, M.S.

The University of Texas at Arlington, 2012

Supervising Professor: Jian Yang and Kytai Nguyen

Abdominal adhesion is a prevalent, troublesome condition occurring after surgical procedures and can cause a variety of side effects such as, abdominal pain with a highly associated cost ($1.3 billion annually for) for expensive surgical removal. Many companies and research groups have studied and developed techniques to prevent adhesion after surgery; however, none have been completely effective or practical for use. Current materials have many drawbacks, such as the inability to degrade, poor surgical handling, and attracting bacteria. Up to 93% of patients receiving abdominal surgeries will develop abdominal adhesions, and thereby a viable treatment option needs to be developed to relieve patient symptoms.

Many studies have established membranes as being the most effective form of material to prevent adhesions; serving as physical barriers to permit separated regeneration

of the mesothelium, and allowing for healing without adhesion. In this study, a synergistic combination of poly(ε-caprolactone) (PCL) and biodegradable photoluminescent polymer (BPLP) will be blended to counteract the drawbacks of current abdominal adhesion materials and to create a new material superior to currently available materials. Several studies were performed to evaluate the potential use of the developed material for anti-adhesion.

First, the PCL/BPLP (PCL10BPLP3) membranes were fabricated using electrospinning technique. PCL only (PCL10) membranes were used for comparison. Various electrospinning parameters and hexafluoroisopropanol (HFIP), as a solvent, were used for fabricating fibers with controlled diameter and pore size.

Second, physical, mechanical, *in vitro* cytocompatibility and antibacterial properties were evaluated for our electrospun meshes. The physical properties of the PCL10BPLP3 mesh were found to consist of strong, elastic mechanical properties similar to that of PCL10 as well as hydrophilic surface properties. From *in vitro* degradation studies, PCL10BPLP3 was degraded at a much faster rate than PCL, with BPLP expediting the degradation rate of PCL. Both PCL10BPLP3 and PCL10 meshes were cytocompatible. When tested using an *E.Coli* bacterial model, the PCL10BPLP3 mesh elicited considerable antibacterial property, whereas PCL10 did not.

Third, the membranes were evaluated for anti-adhesion performance after implantation in the rats' abdomen *in vivo*. It was observed that PCL10BPLP3 had less adhesion on the surface of the mesh compared to the PCL10 sample. Histological results

indicated that PCL10BPLP3 had less inflammatory response and thinner fibrous capsule than other samples.

In general, results from various studies conducted on the membranes indicate the viability and performance of using PCL10BPLP3 mesh for anti-adhesion applications. This membrane holds promising results for adhesion prevention in patients and has potential for clinical usage.

TABLE OF CONTENTS

LIST OF ILLUSTRATIONS

Figure Page

LIST OF TABLES

CHAPTER 1

INTRODUCTION

1.1 Background of Post-Surgical Adhesion

1.1.1 Problems Associated with Post-Surgical Adhesions Occurring within the Body

In a 2001 clinical study, it was found that more than 90% of patients having abdominal surgeries developed abdominal adhesions [1]. Not only are abdominal adhesions cumbersome, but they can also be costly. In the United States alone, abdominal adhesions attribute to over $ 1.3 billion in patient costs for treatment [2]. Many of the procedures that cause adhesions in the peritoneal cavity are common surgeries, such as laparoscopy, colon cancer treatment, hernia repair, and weight loss surgery [3, 4]. Often times during procedures, tissue invasion by surgical instruments, poorly treated or desiccated organs in the peritoneal cavity, thrombosis, and/or surgical material contact with organs occur and accidentally create abdominal adhesions [5]. Unless these incidents do not occur in the peritoneal cavity during surgery, abdominal adhesions are more than likely to form. Permanent abdominal adhesions within the body can cause a multitude of side effects and issues for patients. Not only can adhesions cause bodily pain, but also, infertility in females, difficulty in future operations in the abdominal area, and prohibition of normal intestinal function (blockage) [3, 4]. Depending on the location of the adhesion, the intestines may be tugging against other organs or tissues and prevent digestive flow. The natural

environment in the peritoneal cavity is ultimately disturbed, as adhesions create abnormalities in the structure and function of the abdominal contents [5].

1.1.2 Post-Surgical Adhesion

Abdominal adhesions are essentially scar tissue formations created in the peritoneal cavity due to a variety of external causes/wounds [6]. During operation, there are several different causes of adhesion, which include: bacterial growth, distress, and invasion of particles not natively found in the body [7]. In order for the wound region in the abdomen to heal, mesothelial regeneration and synthesis of fibrotic inflammatory response contents begin to take place [8]. The inflammatory process of abdominal adhesions is initiated within 3 hours after trauma occurred. Although some wounds will begin to heal within 3 days of when the wound occurred, the wounds will remain permanent if breakdown of fibrin or removal of the pre-mature adhesion does not occur quickly enough [9]. For post-surgical abdominal adhesions, this is often the case. Fibrinolysis, that would otherwise normally digest and remove fibrin from the wound site, is locally suppressed as a result of the trauma [10].

To begin, the contents of the abdominal adhesions will first be discussed. Essentially, an abdominal adhesion is initiated by the inflammatory response and release of fibrin-containing exudate [11]. Next, the fibrin, transported by the exudate into the wound region, will begin to deposit at the wound site, followed by fibroblast and collagen influx. Once collagen has entered the wound site, maturation begins to take place, which will ultimately establish collagen bridge formations within the peritoneal cavity [12]. Over time, these collagen bridge formations created by

accumulations of fibroblasts will begin to vascularize and establish eternal adhesions [6] .

Fibrin, created by fibrinogen, is characterized and known as a hard protein [13, 14]. This protein is considered to be insoluble and is primarily excreted for inducing blood clots. After trauma or wound is created within the body, fibrinogen turns into fibrin at the wound side via thrombin and is enlisted to terminate bleeding [14, 15]. In abdominal adhesions, fibrin is present due to trauma or wound that occurred during surgery. Collagen, a fibrous protein, is produced by fibroblasts accruing at the wound site. Collagen maturation into bridges (within the peritoneal cavity) allows for joining of tissues within the cavity that have never been adhered together before [5, 12].

From the pathological and physiological perspective, it seemingly appears as if abdominal adhesions created within the peritoneal cavity are simply wound healing mechanisms that should not be interfered with. However, the scar tissue that forms within the peritoneal wall is more than just a healing mechanism; it is the cause of many dangerous and life-changing side effects and must be treated properly.

1.2 Current Post-Surgical Anti-Adhesion Materials

Over the past few decades, many studies and corporations have focused on developing materials or drugs to prevent peritoneal adhesions. Although some products have been approved by the Food and Drug Administration (FDA) or have promising results, there is currently no fully effective treatment option for prevention of abdominal adhesions [16]. In this section, various materials and drugs are investigated in further detail and the disadvantages of each are described.

1.2.1 Gels

Several studies have developed gel-like materials to be used for preventing adhesions in the peritoneal cavity. Lauder and associates have fabricated a chitosan-dextran gel for adhesion prevention. Essentially, a solution of chitosan and dextran is cross-linked and injected into the wound region in the abdomen (eliminating the need for suturing). Although initial studies appeared promising, there was still some adhesion formed at the location of gel injection [17]. Also, chitosan gel has been reported to disappear by flowing away from the wound site [18]. Another gel-like material that functions as an anti-adhesion material is polyethylene glycol (PEG). This commercialized system, also known as Spraygel®, is a system that contains two different PEG liquids (Confluent Surgical, Waltham, MA). This material is essentially sprayed onto the wounds in the peritoneal cavity and turns into a gel once inside the body. Although studies have shown that Spraygel® has high potential, the product has not been approved by the FDA [10]. Intergel™ is a gel material composed of 0.5% ferric hyaluronate gel available in the United States for preventing post-surgical adhesion (Lifecore Biomedical, Chaska, MN) and has been approved by the FDA since 2001 [19]. Although this product is available for use, clinical trials have shown inefficacy for post-surgical anti-adhesion purposes. In addition, Intergel™ was recently recalled (August 2012) due to adverse side effects in patients such as peritoneal adhesions and pain. Also, it was found that the rate of infections in female patients that received Intergel™ was higher than in female patients that had not received anti-adhesion materials [20]. A major disadvantage of using gels is that the material allows

for extensive cell penetration, prohibiting the tissues on either side of the gel to properly heal and regenerate. It is generally believed that the best method of preventing abdominal adhesions from occurring is to physically separate the tissues that would have otherwise adhered [21].

1.2.2 Drugs

Drugs have been studied for averting adhesion development in the peritoneal cavity [22, 23]. Originally, corticosteroids were assessed for preventing post-surgical adhesions. Pathologically, corticosteroids prevent adhesions from forming based on blockage of the inflammatory response. This would include the initial process of adhesion formation: fibrin deposition and eventual collagen bridge/vascularization formation [24]. However, studies that have tested corticosteroids for efficacy reveal a "catch-22" situation when applying to patients. Although corticosteroids may prevent adhesions from occurring, prevention of wound healing on injured tissue surfaces also occurs [25]. In addition, side effects such as a weakened immune system or pain in bones/muscle can occur after corticosteroid treatment. Since the drug itself is a steroid, it not only causes the physical side effects previously described; it has also been noted to cause mental instabilities in patients [26]. Non-steroidal-anti-inflammatory drugs (NSAIDs) have been used to combat the inflammatory response from taking place in the body. NSAIDs, also commonly as ibuprofens, prevent contents from the inflammatory response, such as leukocytes, from properly functioning [27]. However, several studies have been conducted to analyze the benefits of using NSAIDs and none have yielded reproducible or effective outcomes for anti-adhesion potential [16].

Current studies have yet to obtain results proving the efficacy of drugs for prevention of abdominal adhesions while promoting isolated healing at wound sites [28].

1.2.3 Films

In addition to gels, films are another type of material currently being developed for anti-adhesion purposes. Seprafilm™, a commercially approved hydrophilic anti-adhesion film (Genzyme, Cambridge, MA), is composed of sodium hyaluronic acid (HA) and carboxymethylcellulose (CMC) [29, 30]. Although the FDA approved this film for patient use in 1996, results in clinical trials have not yielded evidence for total adhesion prevention [10]. While reduced, there is still adhesion formation in patients that received Seprafilm™ [31, 32]. Surgeons have also noted the difficulty in handling Seprafilm™ [1, 33, 34]. One film that has yielded promising results is a combination of polygalacturonic acid (PGA) and 1-ethyl-3-(3-dimethylaminopropyl)carbodiimide crosslinker (EDC). According to Lee and associates, the combination of PGA/EDC has been shown to decrease the occurrence of abdominal adhesions in laboratory animals compared to the commercially available Seprafilm™. PGA/EDC degrades at a slower pace than Seprafilm™ [35]. However, fabrication of cross-linked PGA is difficult, which can be unwieldy for high volume production. Additionally, 1-ethyl-3-(3-dimethylaminopropyl)carbodiimide is a cytotoxic chemical. Thus, PGA/EDC films may not be good candidates for replacing Seprafilm™. Alginate films have been studied for use in preventing abdominal adhesions as a barrier. However, this material turns into a gel when implanted within the body, should not be wetted prior to implantation, and can not be implanted into desiccated regions [36, 37]. In general, most films that are

currently in use lack the mechanical properties necessary for handling during surgery. Often times, films are reported to be to brittle and lack the strength needed for suturing, if necessary [30, 31].

1.2.4 Membranes

It is generally accepted among researchers that implanted membranes in the wound site region is the best and most popular form of material for preventing adhesions from occurring [21, 38]. Membranes differ from films in that they have been noted to be easier for surgeons to handle/suture in the body and not brittle. Interceed™ is a commercially available membrane (Gynecare, Somerville, NJ) made of oxidized regenerated cellulose (ORC) and was approved by the FDA for patient use in 1998 [39]. After implantation into the body, this membrane turns into a gel-like substance. Although Interceed™ has been shown to prevent abdominal adhesions from forming, blood must be completely removed from the injury site before applying to work [40]. Blood contact would allow fibrin to deposit on the membrane and adversely produce adhesions [41]. It is undesirable and difficult for surgeons to create a bloodless environment in the patient's body. Thus, the difficulties from this material have made this membrane unfavorable for use during operations [34, 42]. Polytetrafluoroethylene (PTFE) membranes have also been studied extensively for their prevention of adhesion [43]. This material, also commonly known as Teflon®, is a viable option that can be used to prevent adhesion from occurring within the peritoneal cavity. However, a major issue with using PTFE is the lack of biodegradability [21]. In other words, if this membrane is implanted within the body, then an additional operation must be conducted

to remove the membrane from the body [44]. Having to perform another surgery on the patient is quite unfavorable. Bolgen and colleagues performed a study that investigated the anti-adhesion functions of electrospun polycaprolactone (PCL) membrane. Although their findings did not suggest anti-adhesion performance from PCL alone, they noted that the handling and physical characteristics of the membrane were desirable for surgeons [21].

1.3 Our Strategy to Prevent Abdominal Adhesions

1.3.1 Rationale

To conquer the limitations of current materials for anti-adhesion purposes, there are many factors that must be addressed. Most importantly, the material should be biocompatible, biodegradable, and easy to handle [8, 45]. The best form of material for anti-adhesion applications is a physical block, like a membrane [21, 46]. A membrane is superior to the other materials forms by allowing injured sites to remain physically separated, while permitting each site to heal individually without contact [8]. It is critical that wound sites remain separated to prevent adhesion. Additionally, membranes offer better handling and control during implantation for surgeons [30].

In order to have an advantage over current commercialized anti-adhesion membranes, the efficiency of preventing adhesions must be higher [21]. To achieve superiority over current methods, there are several different characteristics that must be considered before fabricating the membrane, which include the material, surface, mechanical, and biocompatible properties. For the purposes of implanting the membrane into the body, the material should have 1) strong and elastic mechanical

features [43, 45]. The mechanical properties of PCL have been reported as excellent with an approximate tensile strength of 2.4 MPa [47]; thus, it is favorable to have a membrane with mechanical properties that does not deviate from the mechanical property values of PCL itself [21]. In addition, the material should present 2) hydrophilic surface properties [48]. As discussed in Section 1.1, adhesion is initiated by an inflow of fibrinogen turning into fibrin at the wound site and inducing thrombosis. It has been found that fibrinogen does not favor adhesion to hydrophilic surfaces, but rather hydrophobic surfaces [49-51]. A surface is considered to be hydrophilic if the contact angle is less than 65^{o}; thus, the lower the contact angle is below 65^{o}, the more desirable the membrane for anti-adhesion purposes [52]. Due to energetically favorable hydrophobic-hydrophobic interactions between fibrinogen and the hydrophobic surface of the membrane, adhesion would, in fact, be promoted on hydrophobic surfaces [53-56]. The material should be 3) biodegradable. For instance, a major disadvantage of current commercialized polymers, such as PTFE, is the inability to degrade within the body, and thus, a need for an additional surgery to remove the membrane [43]. To avoid this, the material to be used for membrane fabrication should be degradable within the body without release of toxic byproducts harmful to the body. Since PCL is slowly degrading polymer, it is ideal to have a membrane with a degradation rate faster than PCL itself [21]. Current commercialized and studied membranes typically degrade within 28 days [57, 58]. In addition, it would be desirable if the membrane had a 4) slight antibacterial property as this may help prevent adhesion that may occur from

possibly invaded bacteria [59]. A very important factor that must be assessed prior to studying the membrane *in vivo* is to test for biocompatibility *in vitro*.

Since it has been concluded that a membrane is the optimal form of material to use for preventing adhesions, the method of fabrication and properties of the membrane should be taken into consideration next. To begin with, there are different ways to create a membrane: by casting, foaming, or electrospinning. Casting involves placing the polymer solution in a mold with a favorable shape and allowing the solvent to evaporate (leaving behind a dry membrane). Foaming involves use of high-pressure gas for the purposes of creating the membrane. Casting and foaming do not provide the membrane with excellent mechanical properties viable for membranes. In addition, by conducting the casting method, organic solvents may be left behind in the membrane, proving to be cytotoxic [60]. None of these fabrication methods offer highly controllable features necessary for creating an anti-adhesion membrane like electrospinning. For instance, the researchers are able to control the diameter and pore size of the membrane [61]. The diameter of the membrane (nonwoven) should provide adequate surface area and small pore size to prevent adhesion from penetrating through the material [30]. The therapeutic agents can easily be incorporated in the membrane using the electrospinning method.

1.3.2. Polymer Selection: Aliphatic Biodegradable Photoluminescent Polymer (BPLP-Ser) and Poly(ε-caprolactone) (PCL)

To suit the needs required for producing an anti-adhesion membrane, a blend of two polymers, BPLP and PCL, are used. BPLP is an exclusive polymer that is biodegradable, biocompatible, and synthesized from citric acid, 1,8-octanediol, and L-

serine. Using monomers from these three products offers a relatively low-cost fabrication. BPLP provides many of the desirable characteristics required for fabricating an anti-adhesion membrane, such as hydrophilic property, a quick degradation time, cytocompatibility, and antibacterial property. In addition, BPLP is fluorescent with an emission range of 303-725 nm (with L-serine side addition), which has potential for imaging *in vivo* degradation [62]. PCL is soft, biocompatible elastic polyester that is most commonly used for long-term applications [21]. Since PCL can take up to 2 years to degrade completely in the body [63], it needs to be combined with another component for faster degradation. Hence, adding BPLP to PCL will create a synergistic combination of materials for anti-adhesion purposes.

For fabrication, it is important to note that BPLP cannot be electrospun alone. BPLP has a low molecular weight at M_n~1000-1500 Da [62], unsuitable for achieving fibers using electrospinning techniques [64]. However, PCL (used in this study) has a molecular weight at M_n~70,000-90,000 Da. PCL is able to be electrospun with relative ease; thus, by blending with BPLP, these two polymers can be electrospun together. Additionally, the fast degradation property of BPLP (22 days) [62] can be used to facilitate more rapid degradation if combined with PCL to form composite fibers. Since PCL is a hydrophobic polymer, modifications must be made to create a hydrophilic surface on the membrane [21]. With the supplement of BPLP, the membrane will become hydrophilic, provide inhibition of fibrotic tissue responsible for causing peritoneal adhesions, and deliver antibacterial properties to the mixture membrane.

Creating an optimal blend of both polymers is essential. Concentrations of each polymer must be carefully tuned before *in vitro* and *in vivo* studies. When choosing the optimal concentration, there are many factors that must be deliberated such as: quick fabrication, small fiber diameter/pore size, cytocompatibility, hydrophilic surface properties, excellent mechanical properties, and quick degradation. PCL can be electrospun easily, contains mechanical properties desirable for handling, and is highly cytocompatible. However, using too much PCL in the polymer solution could compromise fast degradation, hydrophilic surface properties, and small diameter/pore size. BPLP offers fast degradation and hydrophilic surface properties but, in excess, can destroy the mechanical integrity of PCL, quick fabrication, and cytocompatibility. A balance between the two polymers must be determined through pilot studies.

1.3.3 Technique Selection: Electrospinning

Electrospinning is a technique used to fabricate fibers by applying a high potential electric field to a polymer solution [65]. Figure 1.1 illustrates the electrospinning setup.

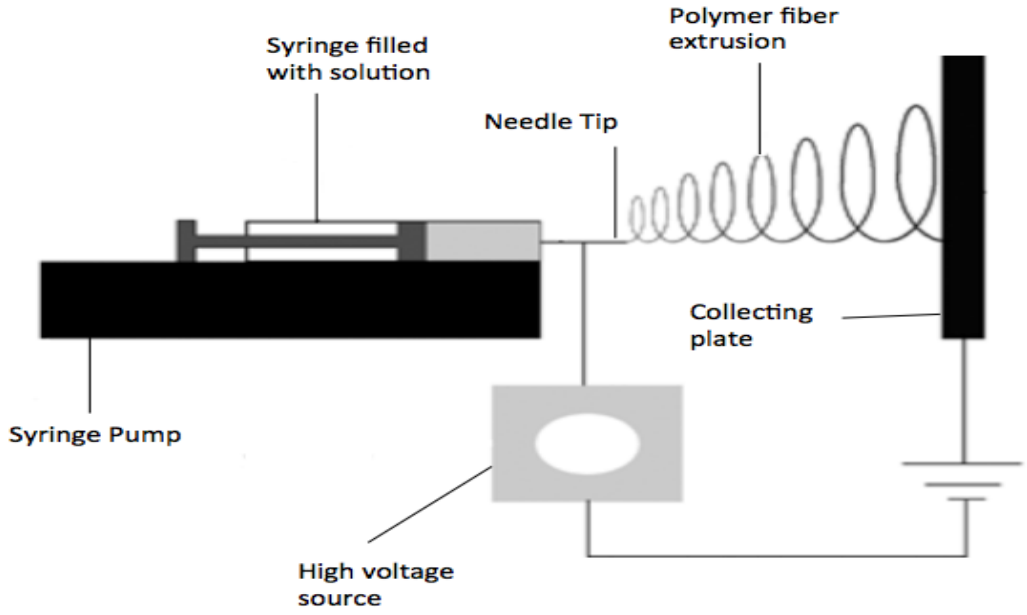

Figure 1.1 An illustration of typical electrospinning setup.

Essentially, the syringe pump holds the syringe filled with the solution to be spun. As the solution is released, the high voltage source imposes an electric potential on the polymer solution, causing the small amount of solution extracted to form into fibers [65]. The fibers travel to the collecting plate with opposite polarity to the charged fibers being extruded [66].

Electrospinning technique for forming nanofibers has been developed over the last decade and offered many opportunities in various fields. The different fields electrospinning could be used for are: criminal justice (protective clothing), safety cleanup (adsorbent materials), and medical (wound dressing) [65, 67]. Formhals patented the electrospinning process in 1934 for the purposes of fabricating micro- to nanoscale fibers [68, 69]. Prior to patenting electrospinning, there were many failed attempts vying for the same purpose, including: fiber drying and collection. In recent

years, many studies have been conducted to optimize fiber fabrication. There are different manipulations with electrospinning parameters that can be adjusted to obtain desired fibers. For instance, Doshi and Reneker found that fiber diameter could be decreased if the distance between the collection and the solution is increased [70].

Electrospinning is the optimal method for fabricating the anti-adhesion membrane. As previously mentioned, casting or foaming are also options that may be considered for fabricating the membrane. Although these two techniques are traditionally used to fabricate other type of membranes, electrospinning is superior to these methods [21]. Electrospinning gives the researcher control over the characteristics desirable for creating a particular membrane [71]. Certain properties of a membrane may need to be manipulated for a certain application such as, pore size or surface area-to-volume ratio [61, 72]. In the case of anti-adhesion membranes, a smaller pore size and greater surface area-to-volume ratio would be beneficial to prevent adhesions from penetrating through the membrane. Electrospinning provides the controllability required for specific applications. In addition, membrane fabrication time is relatively quick depending on the type of solvent used [73]. For this project, electrospinning technique will be used for fabricating the anti-adhesion membranes.

1.4 Project Prospective

1.4.1 Goals

The major objective in this study is to create a membrane that will prevent abdominal adhesions. Peritoneal adhesions can cause a variety of physically and emotionally painful side effects. It is important to explore and ultimately determine a

solution to prevent adhesions from occurring to improve patients' lives. There have been many studies and companies that have fabricated different types of anti-adhesion materials; however, none have been successful in completely eliminating adhesions nor have they been popular among surgeons. Out of all the materials used for preventing adhesions, membranes (physical barriers) have been found to be the best for reducing occurrence. However, membranes need to also have characteristics beneficial for anti-adhesion purposes; as a result, controllable fabrication is essential for this specific application.

To achieve this goal, three specific aims are followed:

Aim 1: Use electrospinning technique to fabricate a membrane composed of an optimal BPLP/PCL concentration with ideal morphology for anti-adhesion applications.

Aim 2: Analyze the physical, *in vitro* degradation, cytocompatibility, and antibacterial properties of the fabricated membrane *in vitro*.

Aim 3: Evaluate the effectiveness of our fabricated membrane *in vivo* to prevent peritoneal adhesions.

1.4.2 Novelty of the Study

Each of the criteria described for optimizing a newly fabricated membrane have never been attempted before for a single membrane. The first part of this study is dedicated to fabricating a membrane with anti-adhesion properties: BPLP has never been successfully electrospun in any capacity; yet, in this study, BPLP is used for fiber fabrication. For the first time, BPLP will be used for anti-adhesion purposes, and a combination of BPLP/PCL will be fabricated into a membrane. Another novel aspect of

this study is the expedited degradation of PCL fibers, which has been previously reported to have prolonged biodegradability [21].

1.4.3 Successful Outcome Result

Upon successful outcome of this study, the ultimate goal of eliminating peritoneal adhesions is one step closer to being accomplished. Abdominal adhesions can be prevented in many common surgeries, which will ultimately eradicate painful side effects. With the prevention of peritoneal adhesion, patients' quality of life can be dramatically improved, whereas elevated costs and risks of follow-up surgeries to remove adhesions will no longer be an issue. In this study, it is desired that the rate of PCL degradation will be greater with the addition of BPLP as opposed to PCL. If this project is successful, a synergistic combination of properties (physical, cytocompatible, and antibacterial) from BPLP and PCL will prevent adhesions from occurring post-surgery. Based on the information acquired from this study, further advancements into the field of anti-adhesion membranes may be made to provide solutions to patients greatly affected by this troublesome condition.

CHAPTER 2

EXPERIMENTAL

2.1 Materials

All materials and chemicals were purchased from Sigma-Aldrich without further purification. These materials are listed in the following sections according to each experiment conducted.

2.2 Methods

2.2.1 BPLP/PCL Synthesis and Solution Preparation

To create BPLP, first, a 1:1 equimolar ratio of citric acid and 1,8-octanediol were combined together. In addition to these two compounds, L-Serine was added at a 0.2 mole ratio with respect to the amount of citric acid. The final mixture was initially heated at a temperature of 160^{o}C until solution has dissolved. At that point, the temperature was reduced to 140^{o}C for approximately one hour to allow for gradual condensation of the polymer. 1,4-dioxane was added in equal volume to the polymer for termination of the reaction. The polymer was completely mixed with the dioxane for 30 minutes and purified in deionized water by precipitation. After purification, the BPLP was placed in an amber-colored bottle, freeze-dried, and stored in a -20^{o} freezer.

Making the solution for electrospinning required physical blending of BPLP-Ser and poly(ε-caprolactone) (PCL) (Mn= 70,000-90,000 Da). Initially, tetrahydrofuran (THF) was used as the solvent to effectively blend the two polymers; however,

hexafluoroisopropanol (HFIP) was later used for faster fabrication and to optimize the physical properties of the membrane. For this project, two types of membrane were created using different polymer concentrations (in the final solution): one of them consisting of 3 wt.% BPLP-Ser with 10 wt.% PCL (PCL10BPLP3) and another one having 10 wt.% PCL (PCL10). Based on pilot trials, the ratio of PCL to BPLP within the fibers were at 77 to 23, respectively, to meet the criteria ideal for anti-adhesion purposes described in Section 1.3. Integration of the BPLP and PCL was accomplished by stirring the two polymers at 500 rpm on a stir plate.

2.2.2 Electrospinning Membrane Fabrication

The polymer solutions were placed into a 10 mL syringe fitted with a flat-tip needle for consistent fiber expulsion. The syringe was secured onto the syringe pump purchased from Kd Scientific (model 781200, Holliston, MA, USA) and set at a flow rate specific to each polymer solution. For PCL10 with THF, the flow rate was set to 0.04 mL/hr, and for PCL10BPLP3, the flow rate was set to 0.03 mL/hr in order to obtain fibers without beads. For both polymer solutions using HFIP, the flow rate was set at 0.3 mL/hr. For all polymer solutions, the voltage and the distance from the needle tip to the collecting plate was kept consistent at 20 kV and 13 cm, respectively. These parameters are summarized in a more organized fashion in Table 2.1.

Table 2.1 Parameters Used for the Electrospinning Process

Solvent	Polymer ID	Voltage (kV)	Flow Rate (mL/hr)	Distance (cm)
THF	PCL10	20	0.04	13
	PCL10BPLP3	20	0.03	13
HFIP	PCL10	20	0.3	13
	PCL10BPLP3	20	0.3	13

Once the syringe was placed onto the syringe pump, a metal membrane was placed onto the grounded collecting plate for easy removal of the polymer fiber membrane upon termination of the electrospinning process. The voltage source was switched on and tuned to 20 kV. The fibers extruded from the syringe and accumulated onto the collecting plate. After the electrospinning process was complete, the newly formed membrane was left in a well-ventilated hood for complete evaporation of the solvent.

2.3 Physical Properties

2.3.1 Morphology of the Membrane Fibers

Samples were first coated with silver using a sputter coater (Plasma Sciences, Inc., CRC-100 Sputter, Lorton, VA, USA). Scanning electron microscopy (SEM) (Hitachi, S-3000N, USA) was used to examine fiber morphology once the membrane was coated thoroughly. With the images obtained from the SEM, the fiber diameter and pore size distributions were calculated for each type of membrane using ImageJ (National Institutes of Health, Bethesda, MD, USA). Values for fiber diameter and pore size were selected randomly using obtained SEM images for both PCL10 and PCL10BPLP3 membranes.

2.3.2 In Vitro Degradation

Samples from PCL10BPLP3 and PCL10 were obtained and weighed to 20 mg. For each membrane, a total of 5 samples was used and placed into tubes filled with 10 mL of 0.01 M phosphate-buffered saline (PBS; pH=7.4). The samples were incubated at 37^{o}C at various time points. Once the time point had arrived, the PBS was removed from the glass tubes and the samples were washed with deionized (DI) water to remove any extraneous salt from the PBS. The DI water was subsequently removed, and the samples were left to freeze dry for approximately 72 hours. The samples were weighed after completely drying and the percent of mass remaining in the membrane was calculated using the Equation 1 below:

$$Mass\ remaining\ (\%) = 100\% - \left(100\ \%\ x\ \frac{W_{initial} - W_{after}}{W_{initial}}\right) \quad (1)$$

where,

$W_{initial}$ = initial weight of the sample

W_{after} = weight of dried sample at the specific time point

The mass remaining was calculated for each sample, and samples were averaged respective to the type of membrane. ^{1}H-NMR studies were conducted on the PCL10BPLP3 sample before and after degradation at 20 weeks, as well as the PCL10 sample after 20 weeks. To conduct this, approximately 0.20 mg of sample was combined with ~1 mL of deuterated chloroform, and placed into NMR tubes. The results were obtained and analyzed.

2.3.3 Surface Properties

Hydrophobicity on the surface of the membrane fibers was analyzed. A single droplet of HPLC water (5 μL) was placed onto the surface of the both membranes and an image was captured using CAM 200 contact angle software (KSV Instruments, Finland). The average angle was recorded for each membrane.

2.3.4 Mechanical Properties

The elastomer tensile mechanical tests of the membranes were obtained using standards according to ASTM D412a with a MTS Insight 2 Mechanical Tester. Using a 500 N load cell, rectangular-shaped samples (25 mm x 6 mm x 0.6 mm) were elongated to failure at a rate of 500 mm/min. The values obtained for each sample were placed into a stress-strain curve for mechanical analysis. The modulus for each sample was calculated at 10% strain of the initial stress-strain curve slope. A total of 6 samples were used for each type of membrane, and final values of tensile strength, elongation at break, and modulus were averaged for each type of membrane.

2.4 In Vitro Studies

2.4.1 Cell Viability

Five equal size samples of each membrane were used for the cell viability study. The samples were sized to fit a transparent, flat-bottomed 96-well plate (Corning, USA) and placed under ultraviolet light overnight for sterilization. Mouse 3T3 fibroblast cells (ATCC, Manassas, VA, USA) were seeded onto each well containing membrane (as well as 5 wells for control with no membrane) at a density of 7500 cells/well in 200 μL of complete Dulbecco's Modified Eagle Medium (DMEM supplemented with 10% FBS and 1% Penicillin). The cells were cultured onto the membrane and incubated at 37^{o}C with 5% CO_2 for time periods of 1,3, and 7 days. DMEM was replaced every 2 days. Standard MTS assay was used to determine cell viability analyzed by a plate reader at

490 nm (Tecan M200 Infinite, Switzerland) according to the manufacturer's instructions.

2.4.2 Optical Density Bacterial Study using Escherichia Coli

About 24 hours prior to conducting the optical density bacterial study, three colonies of *Escherichia coli* (*E.Coli*) bacteria were cultured in 5mL of Lysogeny Broth (LB), and three samples of 25 mg size of each membrane were placed into 1.5 mL tubes and positioned under UV light to prevent extraneous bacterial growth. After 24 hours of incubation at 37^{o}C and 5% CO_2, the 150µL of the *E.Coli*/broth mixture was transferred into a transparent, flat-bottomed 96-well plate (Corning, USA). A plate reader tested for initial absorbance at 650 nm (Tecan M200 Infinite, Switzerland), and dilutions were made to ensure that the *E.Coli*/broth mixture in suspension with the membrane samples would have an initial absorbance level at 0.01 a.u. For this study, the positive control consisted of a 10% (v/v) solution of Penicillin Streptomycin (PenStrep), while the negative control was *E.Coli*/broth without anything added. Bacterial growth was analyzed at time points of 0, 1, 3, 6, 9, and 12 hours for each type of samples.

2.5 In Vivo Studies

2.5.1 Animal Model

A total of 14 6-month-old female Sprague-Dawley rats weighing approximately 250 g were used for the adhesion analysis. From the total, 10 rats were used for histological analysis with 4 animals used for *in vivo* degradation. All of the animal studies were completed in accordance and approval of the University of Texas at Arlington Animal Care and Use Committee (IACUC). Rats were anesthetized with isoflurane and placed backside down with continuous isoflurane ventilation during operation. After the abdomen was shaved, peritoneal sedations of the rats occurred with inoculations of ketamine (40 mg/kg) and xylazine (5 mg/kg), and a 2 cm incision was

made in the middle of the lower abdomen. Next, the abdominal muscle was separated from the subcutaneous tissue. On both sides of the peritoneal cavity, a surgical defect was imposed, creating wounds in the peritoneal cavity wall until bleeding was observed. Also, intestinal defects were created onto the opposing organs facing the surgical defect on the cavity wall. After the wounds were created, a 2 cm diameter of PCL10BPLP3 or PCL10 rounded-shape membrane was sutured on the injury site. For the control, the wounds were not covered or sutured with any membrane. The rats were sacrificed at different time points (2 and 8 weeks, specified for each study in Section 2.5.2 and 2.5.3) for adhesion analysis and *in vivo* degradation. The abdominal wall containing the membrane or the control at the wounded site were removed and placed into 10% neutral buffered formalin solution for histology.

2.5.2 Histology

For the histological analysis, a total of 10 rats were used. After animals were sacrificed at 2 and 8 weeks, fixed samples excised from the body were rinsed, and dried with series of ethanol. Once dried, the samples were embedded in paraffin wax, and cross-sectioned with 4 microns each. The sections were stained with Hematoxylin and Eosin. Images were collected at 4x, 10x, and 40x magnification.

2.5.3 In Vivo Degradation

Prior to operation, each membrane was weighed. After the animals were sacrificed at 8 weeks, the membrane was excised from the body and cleaned thoroughly with DI water to remove any tissue or bodily substances on the membrane. After proper cleaning of membranes, they were exposed to freeze-drying to remove any remaining liquid or fluid. After complete removal of water, each membrane was re-weighed to determine the weight loss over a period or the degradation rate *in vivo*.

CHAPTER 3

RESULTS AND DISCUSSION

3.1 Characterization of Physical Properties of Electrospun Meshes

3.1.1 Fabrication and Preparation of Electrospun Meshes

Initially, various concentrations of BPLP and PCL were electrospun using THF as a solvent; however, the electrospinning speed was incredibly slow. Often times, beads were visible in samples taken during the electrospinning process, and cell viability was low. Despite the given polymer ratio, THF was not a viable solvent for rapid fabrication due to its low polarity and higher boiling point (66^{o}C). To improve fiber structure and cytocompatibility, PCL10BPLP3 was the final concentration used and compared with PCL10. In addition, HFIP was used due to its high polarity and lower boiling point (58.2^{o}C). The exact parameters used for each type of membrane can be found in Table 2.1 of this text.

3.1.2 Morphology

Different membranes that were analyzed with scanning electron microscopy (SEM) were imaged at a magnification that depicted fiber size in a consistent fashion. Membranes were compared with each type of solvent. Figure 3.1 (A) shows PCL10 using THF, while (B) reveals the PCL10 membrane using HFIP. Figure 3.2 (A) shows PCL10BPLP3 using THF, and (B) represents the PCL10BPLP3 using HFIP.

From the SEM images, it can be seen that the fibers for each polymer blend have smooth, uniform, ultrafine fiber formations without any beads that may contain solvent.

Membranes containing solely fibers (no beads) ensure that extraneous solvent is not present (lingering solvent is toxic).

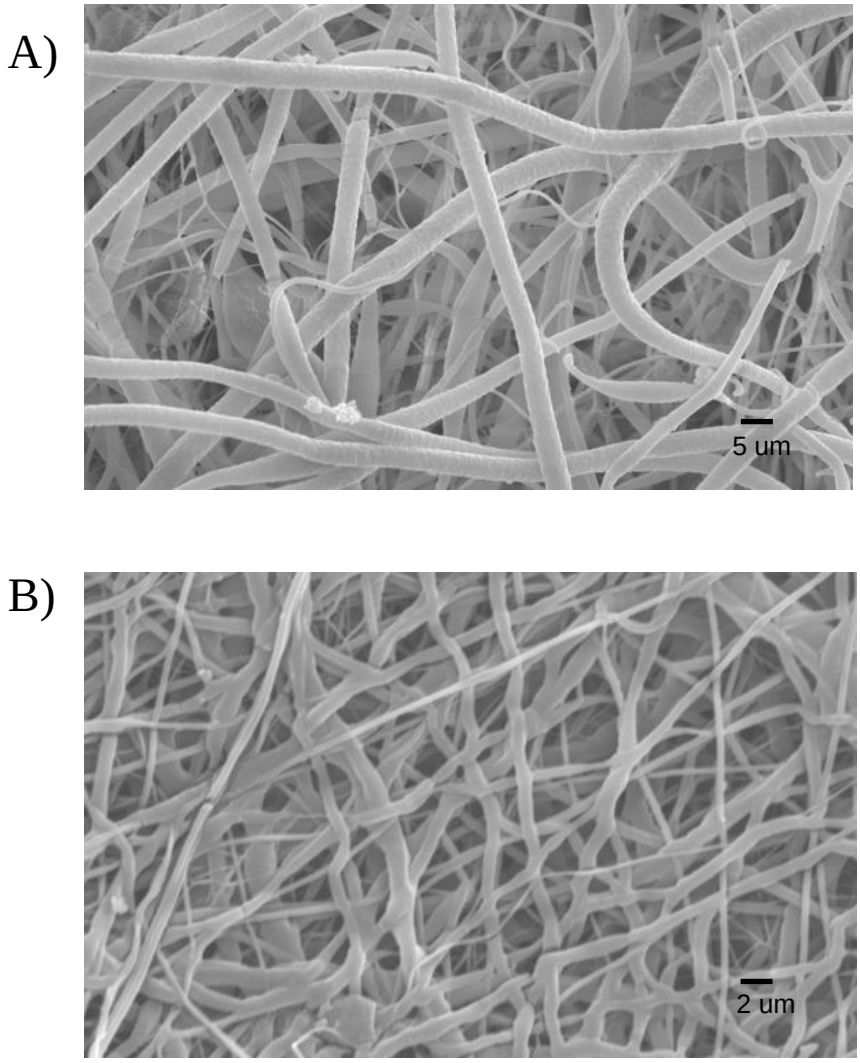

Figure 3.1 SEM micrograph of PCL10 membranes from different solvent (A) THF, (B) HFIP

A)

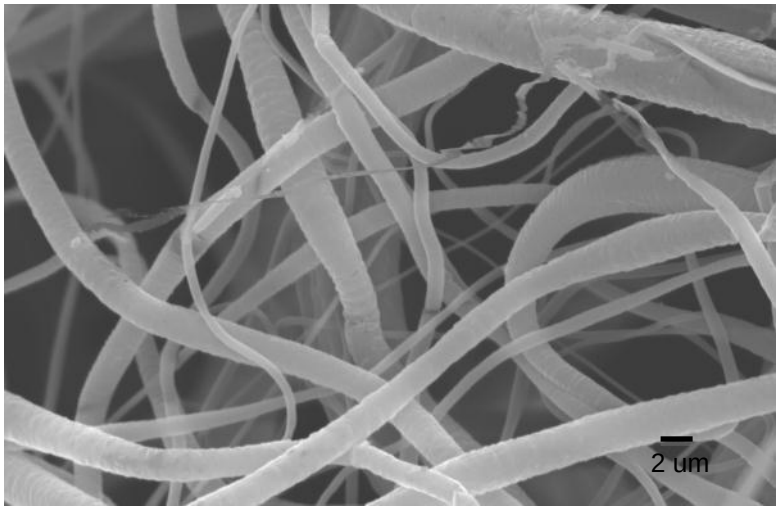

B)

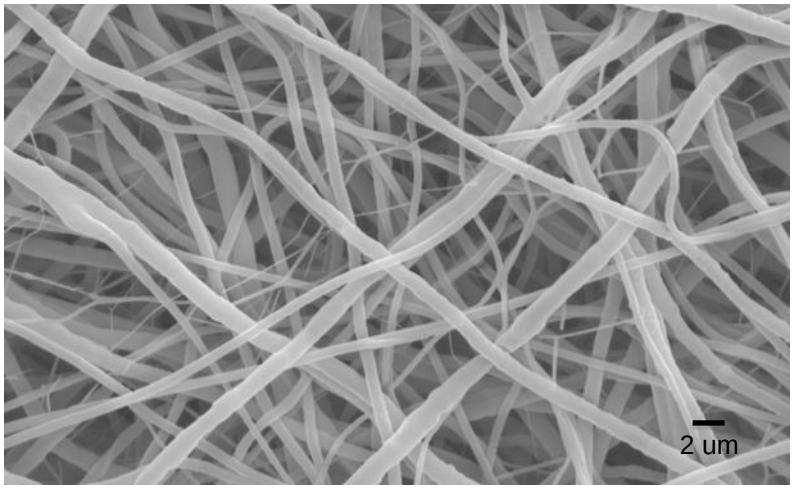

Figure 3.2 SEM micrograph of PCL10BPLP3 membranes from different solvent (A) THF, (B) HFIP

It was also noted that for both PCL10 and PCL10BPLP3 membranes made with HFIP, the fiber formation is denser and less spaced out than membranes made with THF. Once the SEM images were obtained, fiber distributions for each membrane were calculated. Fiber distributions for PCL10 and PCL10BPLP3 membranes can be seen in Figures 3.3 (A) and (B), respectively.

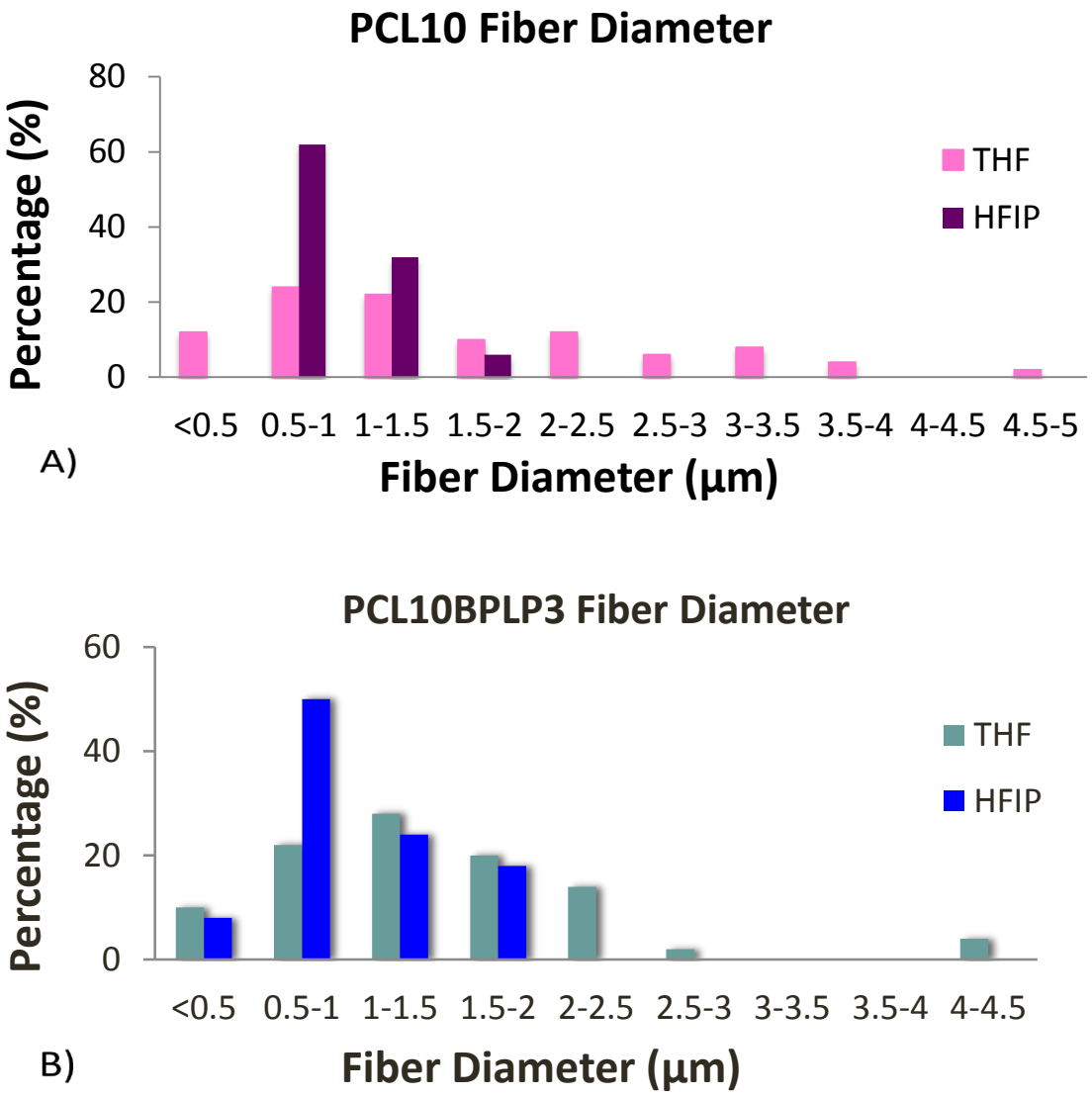

Figure 3.3 Fiber diameter distributions for (A) PCL10 and (B) PCL10BPLP3

The fiber diameter distribution for the PCL10 membrane using HFIP is narrower and more concentrated around the 0.5-2 µm diameter range, whereas using THF leads to a more spread out fiber distribution ranging from <0.5-5 µm diameter range. Likewise for PCL10BPLP3 membrane, using HFIP leads to a narrower fiber distribution, ranging from <0.5-2 µm. However, when using THF, the fiber distribution is wider, ranging

from <0.5-4.5 μm. The average fiber diameter for PCL10 using HFIP is at 0.967 ± 0.323 μm and at 1.63 ± 1.05 μm using THF. The average diameter for PCL10BPLP3 using HFIP is at 1.05 ± 0.433 μm and at 1.44 ± 0.860 μm using THF.

Pore size distribution for each membrane (made with both HFIP and THF) was also calculated. Figure 3.4 (A) represents the pore size distribution relating to solvent type (HFIP or THF) for PCL10 membrane and (B) represents the pore size distribution for PCL10BPLP3 membrane. The pore size distribution for both PCL10 and PCL10BPLP3 using HFIP is narrower than for THF. The pore size distribution ranges from 0-10 μm by using HFIP and 0- >20 μm by using THF. The pore size average for PCL10 using HFIP is 3.14 ± 1.20 μm and 13.2 ± 5.08 μm using THF. The pore size distribution for PCL10BPLP3 ranges from 0-15 μm using HFIP and 0->20 μm by using THF. The average pore size for PCL10BPLP3 is at 5.44 ± 2.88 μm using HFIP and 11.0 ± 4.43 μm using THF.

Meshes that contain microfiber diameters within small, narrow distributions are superior to meshes containing wide distributions for anti-adhesion applications. Based on the results, the membranes fabricated with HFIP appear to be superior to using THF based on the narrower and smaller fiber diameter and pore size distribution. When electrospinning a polymer solution for anti-adhesion purposes, it is optimal to obtain fiber diameters within a close range to ensure a reproducible procedure as well as to obtain a large surface area-to-volume ratio. Figure 3.3 (A) and (B) reveal that meshes made with HFIP have small fiber diameters and narrow distributions.

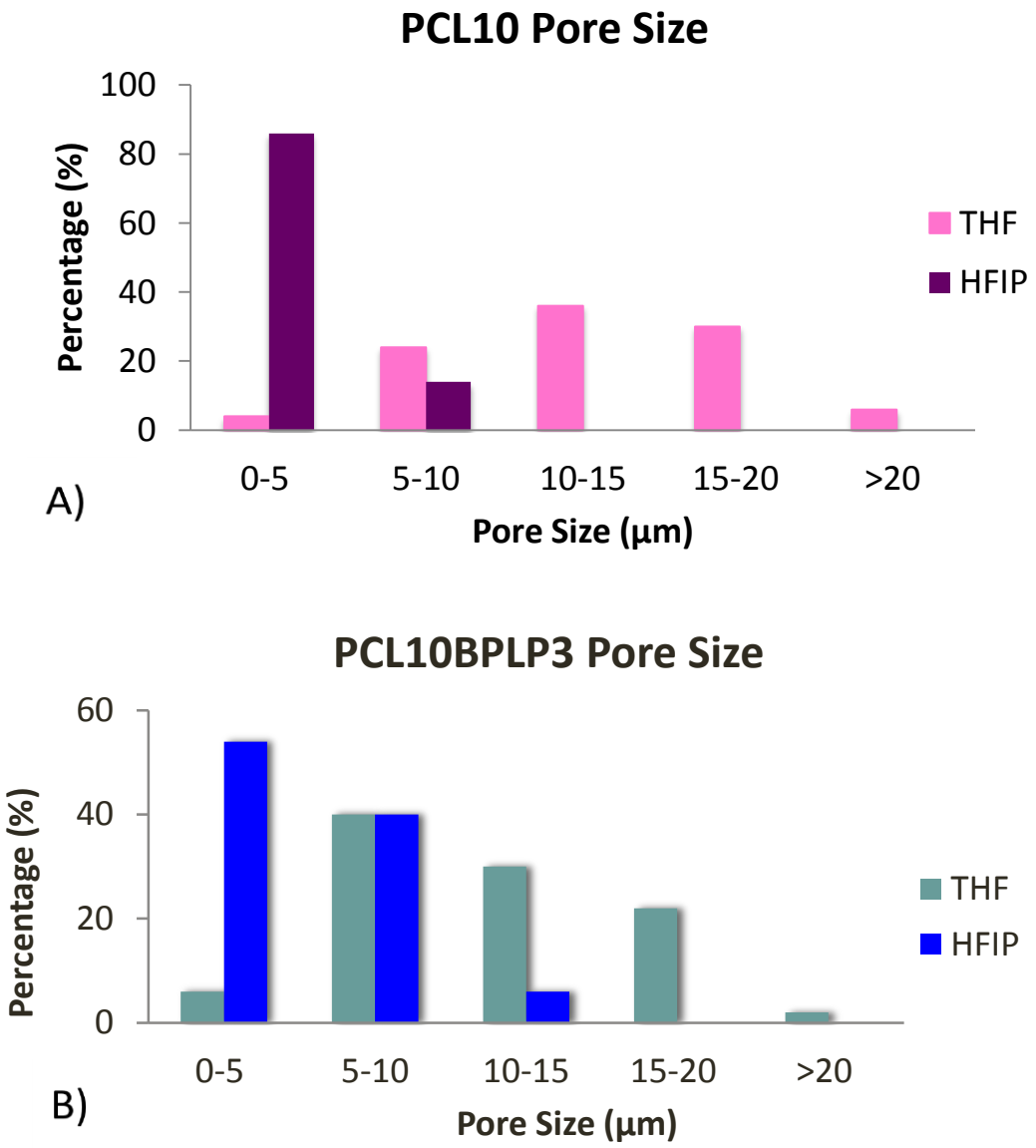

Figure 3.4 Pore size distributions for (A) PCL10 and (B) PCL10BPLP3

Additionally, the pore size should have a narrow distribution to achieve maximum reproducibility of fabrication. Furthermore, if the pore size is not only narrowly distributed but also small, then the membrane is quite suitable for anti-adhesion purposes for preventing penetration of adhesion components. Macrophages initially used for peritoneal regeneration have diameters between 20-30 µm [74], and

with 100% of pore sizes being less than 15 μm, PCL10BPLP3 membrane should prevent a considerable amount of cell penetration. In other words, the membrane should contain a large surface area and small pore sizes to reduce fibrotic tissue formation between the organ and peritoneal wall via the membrane itself. Based on this assessment, using HFIP to fabricate the membranes appears to be best fit for anti-adhesion applications. Figure 3.4 (A) and (B) demonstrate the small pore size and narrow distribution of PCL10 and PCL10BPLP3, respectively. The reason for the difference between fiber diameter and pore size for membranes made with THF and membranes made with HFIP is probably due to the polarity of the latter solvent [73] . Based on the results, the membranes fabricated with HFIP appear to be superior to using THF based on the narrower and smaller fiber diameter and pore size distribution. If the fibers of the mesh have this morphology, then the mesh acts as a "blocker", preventing the fibrotic tissue formation from occurring inside and through the membrane.

3.1.3 In Vitro Degradation Analysis

The degradation for both PCL10BPLP3 membrane and PCL10 membrane in PBS can be seen in Figure 3.5. Essentially, the percent of weight remaining with respect to the initial weight of the membrane is calculated and analyzed at various time points from 0-28 weeks. From the graph, the PCL10 membrane did not seem to degrade a large amount. This can be seen at 28 weeks, where the PCL10 membrane had 93.36% weight remaining, indicating that most of the PCL had not degraded. On the contrary,

the PCL10BPLP3 membrane had 66.40% weight remaining. Thus, the degradation rate of the BPLP-containing mesh was higher than the membrane containing only PCL.

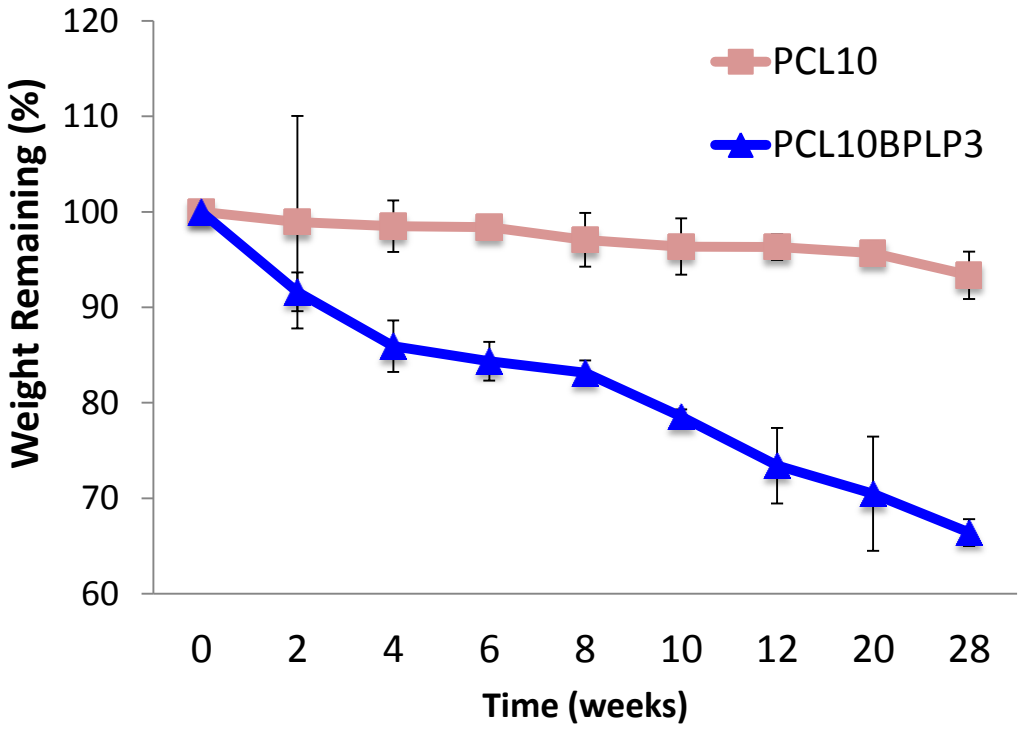

Figure 3.5 *In vitro* degradation of PCL10 and PCL10BPLP3 membranes in PBS

To analyze how the fibers were degrading, SEM images were captured for the meshes after 20 weeks degradation. In Figure 3.6 (A), some fibers from the PCL10 are observed to fragment at various locations along fiber formations. However, these fragments are not as prevalent as fibers from PCL10BPLP3, seen in Figure 3.6 (B). The process in which PCL fibers degrade is by fragmentation [75]. Thus, BPLP helps PCL to fragment more frequently to promote further degradation. It should be noticed that in the PCL10BPLP3 mesh, the fiber formations are fragmenting in the same manner as the PCL10 mesh. This indicates that during the fabrication process of BPLP and PCL, the

two polymers are merely blended physically. There is no chemical bond between the two polymers, but rather a uniform mixture representing a physical combination of the two polymers. In Figure 3.6 (B), it is noted that the locations of blended BPLP are now degraded (red arrows), possibly indicating that BPLP degrades faster than PCL. In other words, each polymer in the membrane degrades in its own manner and time, but the degradation of BPLP expedites the degradation of PCL.

To further explore the degradation mechanism, ^{1}H-NMR was conducted using deuterium chloroform, as a solvent, to determine if any BPLP was remaining in the PCL10BPLP3 mesh after 20 weeks degradation. In order to conclude if BPLP had fully degraded, the peaks obtained from the ^{1}H-NMR spectrum of the PCL10BPLP3 membrane were compared with the peaks from the ^{1}H-NMR spectrum of the PCL10 mesh. If the peaks from the spectrums of each mesh were identical, then it would be concluded that the BPLP had entirely degraded from the PCL10BPLP3 mesh. Figure 3.7(A) shows the ^{1}H-NMR spectrum of the PCL10BPLP3, and (B) represents the PCL10. Each peak is labeled with a letter to depict what chemical structure is represented in relation to the PCL chemical structure seen in Figure 3.8.

A)

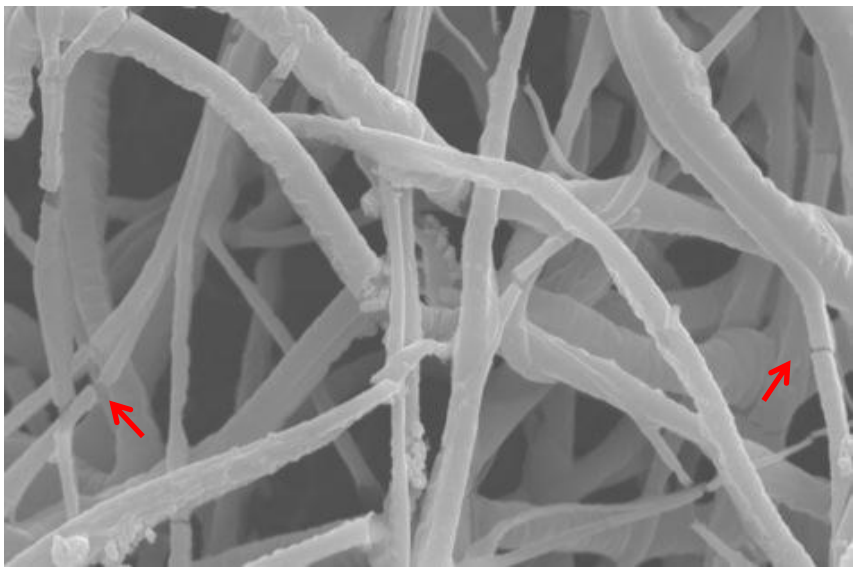

B)

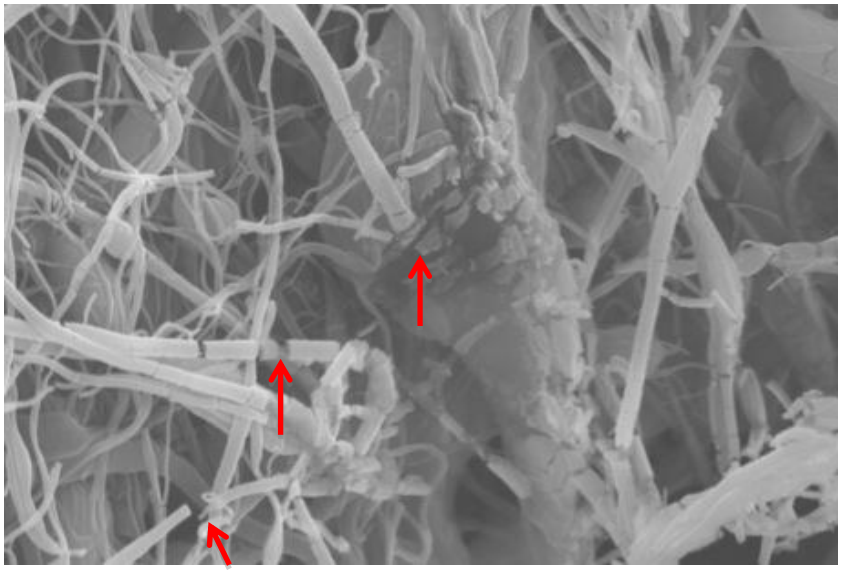

Figure 3.6 SEM images (A) PCL10 and (B) PCL10BPLP3 samples after 20 weeks degradation in PBS

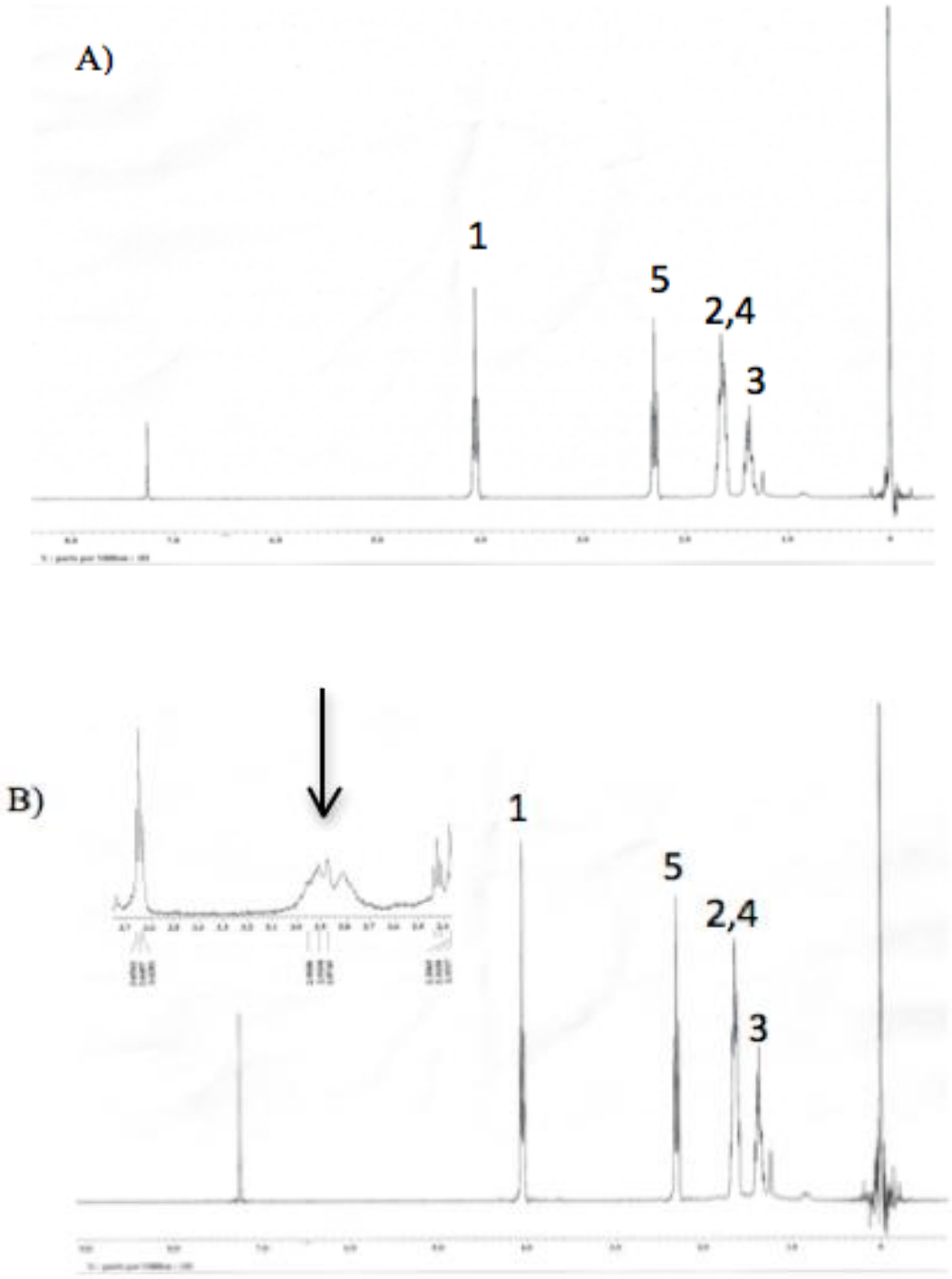

Figure 3.7 ^{1}H-NMR spectrum of (A) PCL10 and (B) PCL10BPLP3 with membranes at 20 weeks degradation time point. Insert at (B) indicates BPLP of PCL10BPLP3 membrane prior to degradation.

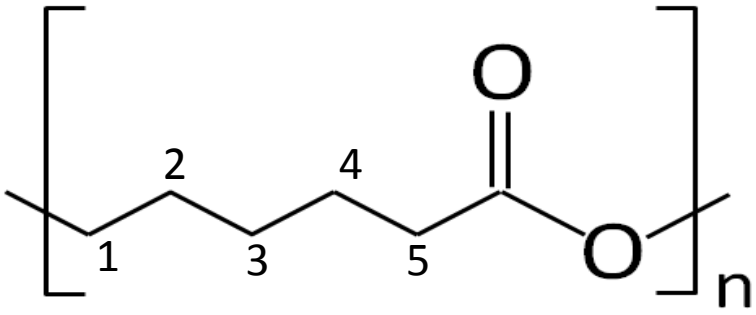

Figure 3.8. The location of the peaks on the chemical structure of PCL.

Based on the ^{1}H-NMR spectrum of each type of mesh, the peaks appear to fall at identical locations. Peaks “2”, “3”, and “4” are assigned to the -CH_2- on the backbone of the PCL polymer chain, located around 1.6 ppm (“2”, “4”) and 1.4 ppm (“3”). The –OCH_2- is assigned to peak “1”, indicated at approximately 4.1 ppm. The –CH_2- is assigned to the peak labeled as “5” at approximately 2.2 ppm. The labeled peaks are assigned to the same functional groups for the spectrums of both PCL10 and PCL10BPLP3 mesh. As a result, this shows that the contents are equivalent for the PCL10BPLP3 mesh and the PCL10 mesh. If any BPLP were left in the PCL10BPLP3 membrane, the peak for citric acid would have appeared around 2.7 ppm [62]. However, it is evident from the spectrum that no peaks were present around 2.7 ppm (Figure 3.7 (B)), indicating complete degradation of BPLP after 20 weeks. An insert is provided in Figure 3.7 (B) that indicates the ^{1}H-NMR citric acid peak visible (arrow) contained in the PCL10BPLP3 membrane prior to degradation. However, in the PCL10BPLP3 membrane, only PCL is in the contents of each type of membrane by the 20-week time point, since the citric acid peak (indicative of BPLP) is not present.

Figure 3.6 (B) reveals the fragmented fibers of the PCL10BPLP3 during the degradation process. However, the extent of fragmentation is greater than PCL10 Figure 3.6 (A), thus, facilitating the theory that BPLP simply helps to expedite PCL degradation via further fragmentation. Thus, the addition of BPLP helps to increase degradation rate of PCL fibers. To quantify this assumption, Equation 2 is used:

$$D_{PCL} = \frac{D_{Total} - \frac{3}{13} D_{BPLP}}{10/13} \quad (2)$$

where D_{total} is the degradation rate of the PCL10BPLP3 membrane, D_{BPLP} is the degradation rate of 3 wt.% BPLP, and D_{PCL} is the degradation rate of PCL fibers within the PCL10BPLP3 mesh.

Table 3.1 lists the values calculated from using Equation 2 above at the time points used for the degradation study. Table 3.1 lists the weight degraded for the PCL10 membrane compared to the weight degraded for PCL10 when BPLP is added (PCL10BPLP3 membrane).

Table 3.1 Comparison of Weight Degraded for PCL10 with 3 wt.% BPLP Added

Time Point (weeks)	Percentage of PCL Degradation from PCL10 Sample	Percentage of PCL Degradation from PCL10BPLP3 Sample
0	0%	0%
2	1.08%	1.08%
4	1.51%	1.51%
6	1.60%	1.60%
8	2.93%	2.93%
10	3.64%	3.64%
12	3.70%	4.55%
20	4.33 %	8.32%
28	6.64%	13.70%

After 10 weeks, the PCL fibers in the BPLP-containing mesh begin to degrade at a faster rate than the mesh not containing BPLP. The value at 12 weeks is 3.70% for PCL fibers only, while 4.55% is the weight degraded for PCL fibers after BPLP is added. At 28 weeks, a more drastic difference is observed: 6.64% weight degraded for PCL fibers in the PCL10 mesh and 13.70% in the BPLP-containing mesh. Prior to 12 weeks, it is predicted that the PCL fibers did not degrade as much as the BPLP, thus, the values for PCL fiber weight degradation were essentially equivalent between the two membranes.

It should be noted that each polymer blended degrades due to hydrolysis, and PCL fiber degradation is increased due to the rapid degradation of BPLP. The purpose of comparison between the two values is to demonstrate the advantages of BPLP

accelerating the degradation rate of PCL fibers. As mentioned in Section 1.2.4, one of the disadvantages of current membranes used for anti-adhesion applications is the inability to degrade within the body. However the PCL10BPLP3 mesh has relatively faster degradation rate, proving to be superior to non-degradable membranes and slowly degradable PCL. Thus, the need for removal after implantation is no longer applicable for the PCL10BPLP3 membrane.

3.1.4 Surface Properties

To test the hydrophobicity of each mesh, water contact angle studies were conducted, as mentioned in Section 2.3.2. Figure 3.9 represents a photograph of the PCL10 (A) and PCL10BPLP3 (B) membranes immediately taken after a 5μL HPLC water droplet was placed on the surface. As can be seen, the water droplet placed onto the surface of the PCL10 membrane maintained a more spherical structure, whereas in the PCL10BPLP3 membrane, the water droplet had absorbed immediately. Using the images obtained from the camera, the average contact angle of each water droplet in association with the membrane surface was calculated. The contact angle was found to be approximately $123.63^{o} \pm 3.13$ for the PCL10 membrane; while for the PCL10BPLP3 membrane, the average contact angle was $0.00^{o} \pm 0.00$ (Values are listed in Table 3.2).

A)

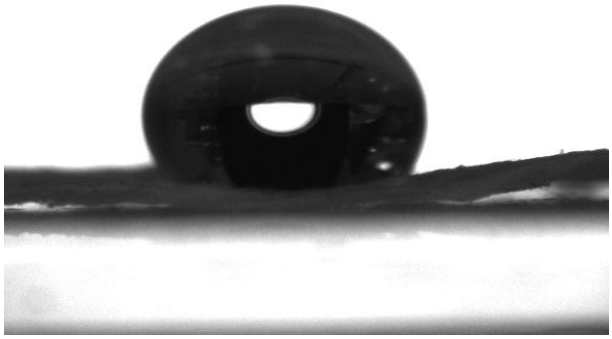

B)

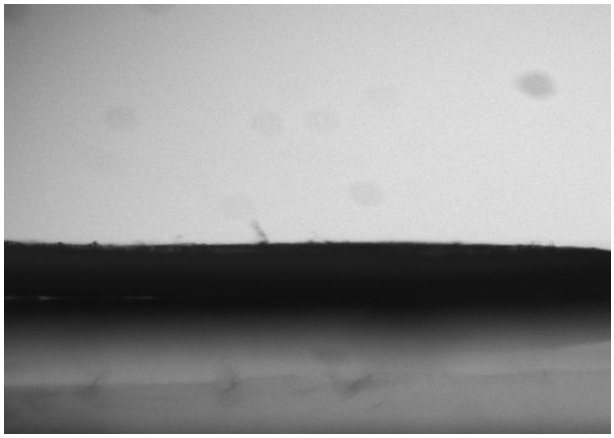

Figure 3.9 Water contact angle of (A) PCL10 and (B) PCL10BPLP3

During the contact angle study, it was noted that the structural integrity of the water droplet placed onto the PCL10 membrane was maintained, while the water droplet had immediately disappeared and absorbed into the PCL10BPLP3 membrane. Based on both the quantitative and qualitative analysis, it can be concluded that the PCL10 membrane has a hydrophobic surface property, while the PCL10BPLP3 membrane has a hydrophilic surface property. This is, in fact, beneficial to anti-adhesion applications. Fibrinogen, known as a hard protein commonly found in the

contents of abdominal adhesions, tends to favor adhesion onto hydrophobic surfaces due to the vast amount of entropic gain from hydrophobic-hydrophobic interactions [53-56]. Thus, in order to prevent fibrotic adhesions from occurring between the abdominal organs and the peritoneal wall, the PCL10BPLP3 membrane proves to be fit.

3.1.5 Mechanical Properties

Mechanical testing for both types of mesh was conducted for comparison between the polymers (Table 3.1). Figure 3.10 displays two representative stress-strain curves for both PCL10 and PCL10BPLP3. The average thicknesses of the membranes were at 600 microns (0.6 mm). Based on the values obtained during the mechanical testing, the tensile strength, elongation at break, and elastic modulus were averaged for each mesh and analyzed. For tensile strength, the value for PCL10 is 2619.20 ± 746.51 kPa and 2462.75 ± 780.25 kPa for PCL10BPLP3. It is noted that the tensile strength of PCL is not significantly altered by the addition of BPLP. The elongation at break was 109.55 ± 6.21 % for PCL10 and 107.93 ± 8.71 % for PCL10BPLP3. Once again, the elongation at break was not significantly different for the PCL10BPLP3 mesh compared to the membrane containing PCL10. Thus, by adding BPLP to the PCL, the strength, elastic modulus, and elongation at break were not significantly affected. For the elastic modulus, the PCL10 had a value of 9.40 ± 1.57 MPa, while the PCL10BPLP3 blend had a value at 14.63 ± 3.12 MPa. The elastic modulus for the BPLP containing mesh was not significantly different than membrane containing only PCL.

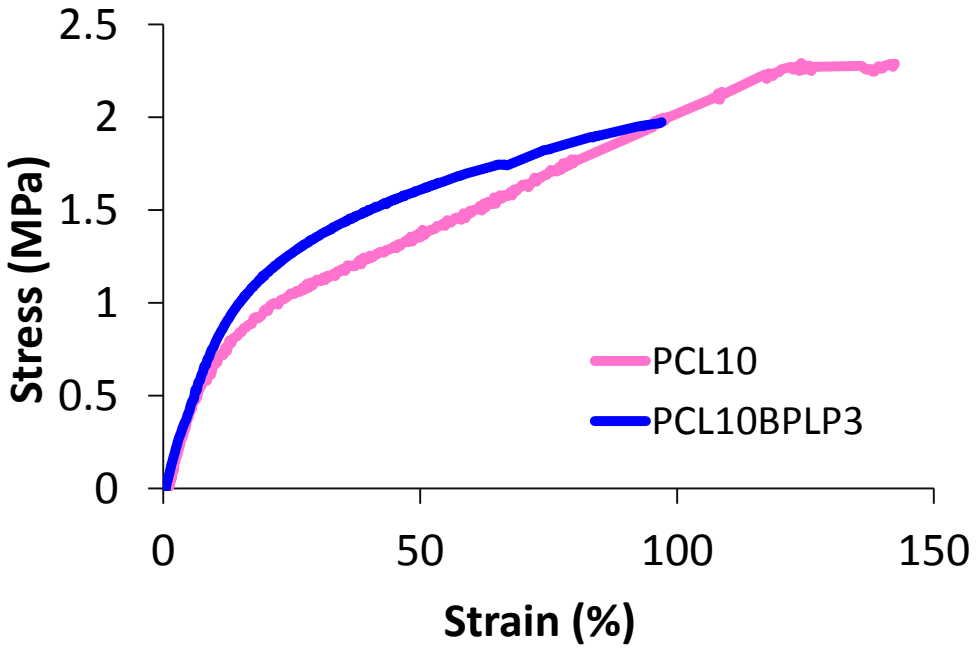

Figure 3.10 Stress-strain curves of electrospun PCL10 and PCL10BPLP3 meshes

Table 3.2 Mechanical and Surface Properties

Sample ID	Tensile Strength (kPa)	Elongation at break (%)	Elastic Modulus (MPa)	Contact Angle
PCL10	2619.20 ± 746.51	109.55 ± 6.21	9.40 ± 1.57	123.63^{o} ± 3.13
PCL10BPLP3	2462.75 ± 780.25	107.93 ± 8.71	14.63 ± 3.12	0.00^{o} ± 0

Although the mechanical properties (besides elastic modulus) between the two types of mesh are not generally altered, the surface properties are different. The addition of BPLP to PCL for the purposes of creating an anti-adhesion membrane is proven to be synergistic. Not only does the hydrophilic surface property deter fibrotic tissue adhesion, but also, the mechanical properties are ideal for surgical handling. The

strength of the membrane is suitable for withstanding forces of motion during bodily movement or suturing, and the elongation at break reveals that the membrane can be stretched to withstand surrounding forces. From the values of the tensile strength and elongation at break in Table 3.1, the PCL10BPLP3 mesh appears to be able to accommodate for bodily movement and surgical application. Since the body is expected to degrade the membrane after proper wound healing, it should possess mechanical properties that allow for accommodation of physical activities during the degradation process.

3.2 In Vitro Performance of PCL10BPLP3 and PCL10 Membranes

3.2.1 Cytocompatibility and Proliferation Study using Mouse 3T3 Fibroblasts

The cytocompatibility of the PCL10BPLP3 membrane with mouse 3T3 fibroblast cells was analyzed using standard MTS assay procedures for the 1-day time point, and cell proliferation was measured for 3 and 7 day time points. Each sterilized membrane was cut into rounded shapes fitted into the bottom of a 96-well plate, and seeded with 7500 cells/well in DMEM. Since the mesh is going to be implanted within the body, it is important that the membrane is nontoxic to cells. After many trials, the concentration of PCL10BPLP3 was selected to have the best cytocompatibility. Other polymer concentrations tested, such as 3 wt.% BPLP / 8 wt.% PCL, did not yield cell viability levels as high as the PCL10BPLP3. It is expected that the PCL10 mesh will have high cell viability and proliferation due to the biocompatibility of PCL. However, too high amounts of BPLP could result in cytotoxicity due to the citric acid content, which might lower the local pH level. On day 1, there is no significant difference

(P>0.05) in the amount of fibroblast cells seeded for each group using T-test; each group had an equal amount of cells, indicating cytocompatibility. The percent of cell viability was at 100% for control, 98% for PCL10, and 97% for PCL10BPLP3. At day 3, cell proliferation is found for PCL10BPLP3 at 119%, and a further cell proliferation increase to 252% at day 7. At day 3, cell proliferation is found for PCL10 at 120%, and a further cell proliferation increase to 235% at day 7. Based on Figure 3.11, there was not a significant difference in cell viability at day 7 between the control and the PCL10BPLP3 membrane (P=.082). Our results indicate that the PCL10BPLP3 mesh is considered to be cytocompatible, and thereby the PCL10BPLP3 membrane is potentially safe to use *in vivo*.

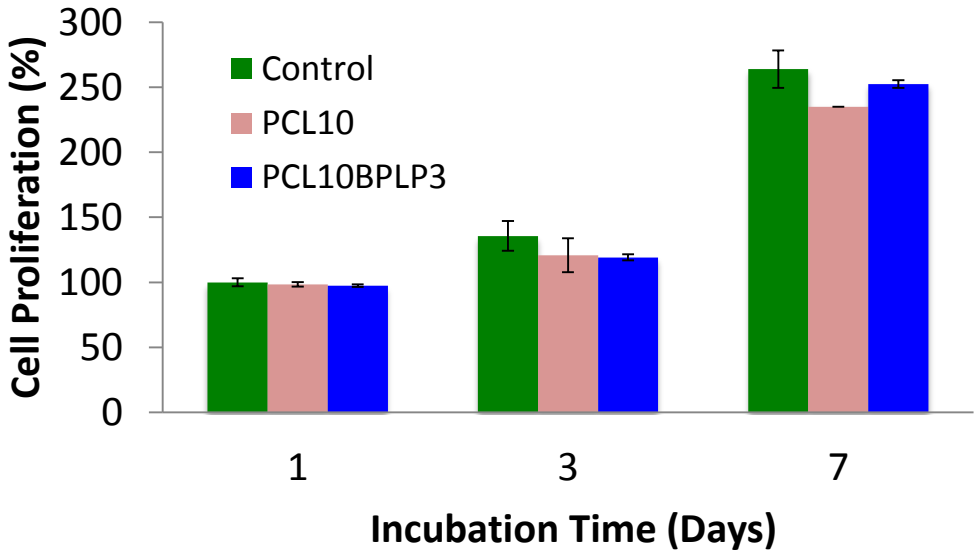

Figure 3.11 3T3 Fibroblast compatibility analysis at various time points for PCL10 and PCL10BPLP3. No statistical difference is observed between Control and PCL10BPLP3 using T-test (P>0.05).

3.2.2 Antibacterial Property of PCL10BPLP3 with Escherichia Coli

Using *E.Coli* as a bacteria model, the antibacterial property of PCL10BPLP3 was analyzed. In this study, *E.Coli* was chosen due to its common presence in the abdomen during peritonitis where the application of the mesh being used [76]. The positive control group featured a 10% (v/v) solution of PenStrep, while the negative control group was bacteria culture not containing anything. The results were calculated after obtaining values from the plate reader and are represented in Figure 3.12. At the initial time point (0 hour culturing time), all of the samples were at the same bacterial level by using T-test. No group had significantly less or more bacteria than ($P > 0.05$) another group. After 1 hour, the PCL10BPLP3 group had significantly fewer bacteria than the Control ($P < 0.05$). In addition, as the time points increased, the PCL10BPLP3 group had significantly less bacteria than the control. Although the antibacterial level of the PCL10BPLP3 mesh was only slight compared with PenStrep, it is statistically significant from the control ($P < 0.05$). In a practical application, using the PCL10BPLP3 membrane as opposed to using nothing is helpful for inhibiting bacterial growth. At the longest culturing time point, 12 hours, the PCL10BPLP3 worked better than the control and PCL10 mesh for preventing *E.Coli* growth.

Bacterial infections or invasions into the body during surgical operations are one of the major causes of infection and post-operative adhesion formations. Bacteria entering the body trigger the immune response, which will ultimately lead to the inflammatory response (adhesion-forming) contents transported to the peritoneal cavity. Since the PCL10BPLP3 mesh is seen to exhibit antibacterial properties and inhibit

infection. Thus, adhesion formation caused by bacteria invading the body should be prevented to a further extent as opposed to using PCL10 or no membrane.

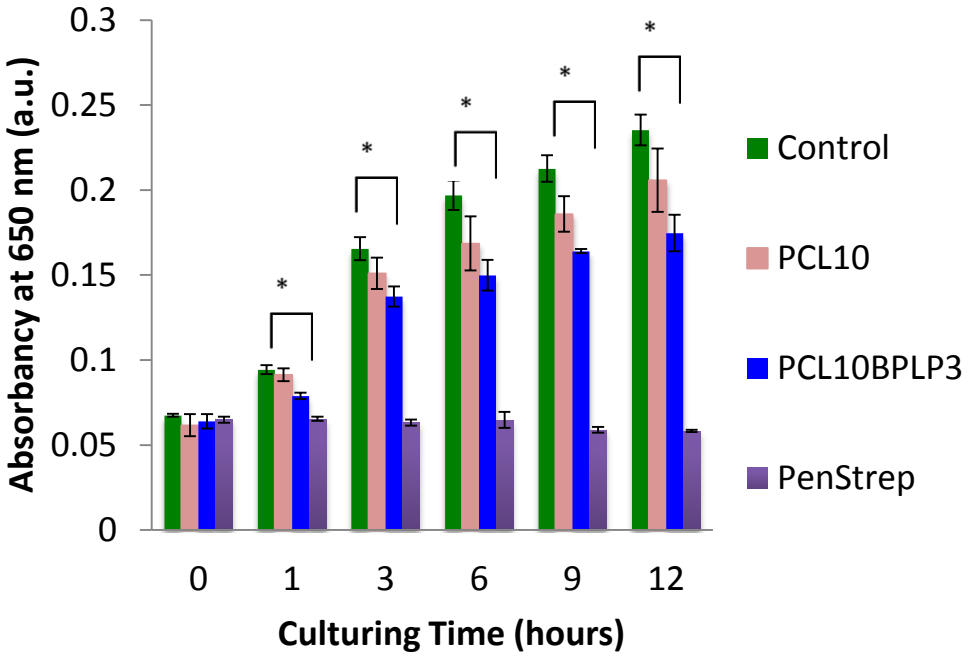

Figure 3.12 E.Coli optical density analysis with E.Coli for each type of membrane. Positive and negative controls are represented as "PenStrep" and "Control", respectively. Significant difference is observed between the PCL10BPLP3 sample and the control ($P<0.05$).

3.3 In Vivo Performance of PCL10BPLP3 and PCL10 Membranes

3.3.1 Animal model

The schematic of the animal model and operation process used for the membrane implantation is illustrated in Figure 3.13. Label "A" depicts the location of the 2 cm abdominal excision. Label "B" demonstrates the isolation of the wall close to the cecum on one side of the excision. Label "C" and Label "D" represent the two sides of the opened excision. "C" indicates the side with the wounds created on the peritoneal

wall and the outer surface of the intestine facing the peritoneal wound site. “D” indicates the side with the membrane sutured over the wound on the peritoneal wall. Figure 3.14 lists an image of the sutured mesh immediately after surgery. This animal model reflects an actual scenario that would occur in the creation of abdominal adhesions. If the wound were created between the organ wall and the peritoneal cavity, the inflammatory response would be initiated to begin the healing process. In the meantime, the organ and abdominal wall will begin to adhere together, similar to actual cases of post-surgical adhesions in patients. The mesh will serve as a physical barrier between the organ and abdominal wall to promote separated mesothelium regeneration.

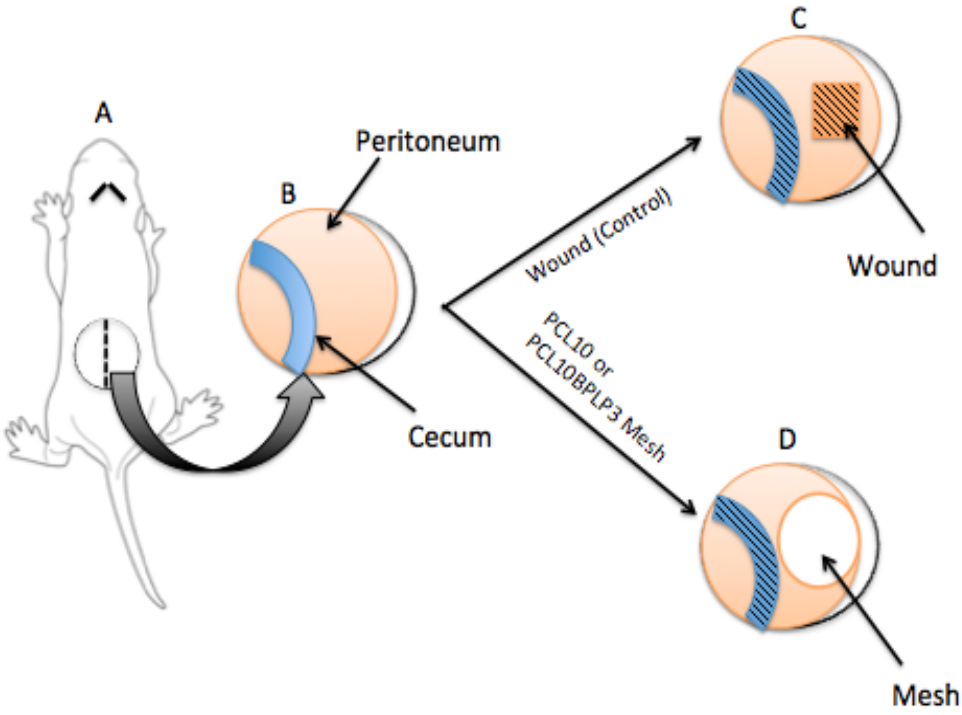

Figure 3.13 Animal model scheme depicting the surgical procedure used to inflict wounds. The vertical lines on the peritoneum and cecum represent wounds created during operation.

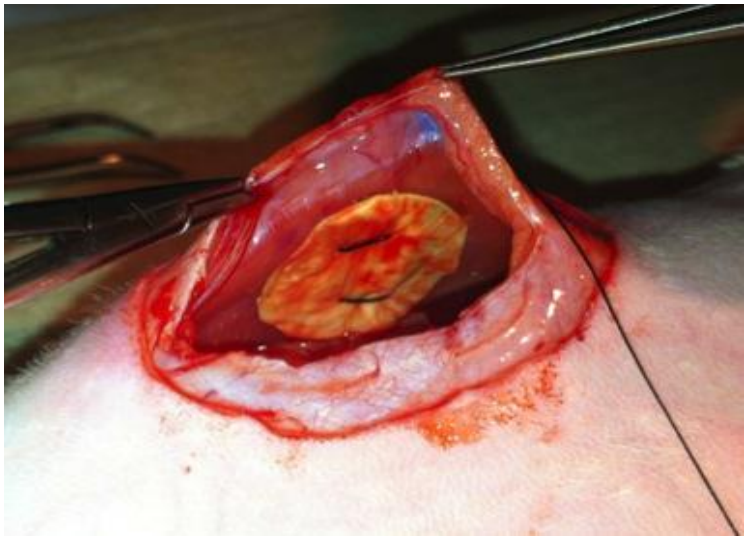

Figure 3.14 Mesh sutured on the abdominal wall after surgery.

3.3.2 Adhesion Evaluation

After sacrificing the animals, adhesion was analyzed at the site of the mesh implantation. The adhesions were evaluated based on a rating or score used as described in Table 3.3. The adhesion scores range from 0 (no adhesion) – 3 (moderate to severe adhesion), depending on the extent of adhesion present. The technique to measure a particular membrane adhesion score is simple; if the animal had no adhesion formation, then the sample (membrane type) was rated as 0, and counted as 1.The total number of samples counted that were rated within a rank were tabulated and placed into Table 3.4 and 3.5 for time points at 2 weeks and at 8 weeks, respectively.

Table 3.3 Ratings Used to Rank the Amount of Fibrotic Tissue Formations on Implanted Membranes

Rating	Definition
(-)	No adhesion formation
(*)	Very slight evidence for adhesions
(**)	Slight to moderate amount of adhesions
(***)	Moderate to severe adhesions

Table 3.4 In vivo Adhesion Ranking at 2 Weeks of Implantation

Membrane	Adhesion Score[1]			
	-	*	**	***
Control	1	3	1	1
PCL10	0	1	2	0
PCL10BPLP3	1	0	2	0

Table 3.5 In vivo Adhesion Ranking at 8 Weeks of Implantation

Membrane	Adhesion Score[1]			
	-	*	**	***
Control	0	2	2	0
PCL10	0	1	2	3
PCL10BPLP3	0	4	2	0

[1]Values are based on the number of samples ranked for each score (each number represents one sample).

The values in Table 3.4 reveal the scores observed for each sample at 2 weeks, indicative of acute adhesion formation. The ranking definitions were determined by the amount of adhesion tissue found on the surface of the mesh (facing the peritoneal cavity and the abdominal organs). Adhesions are evident by the presence of fibrous bands formed at the mesh site as well as blood vessel formation.

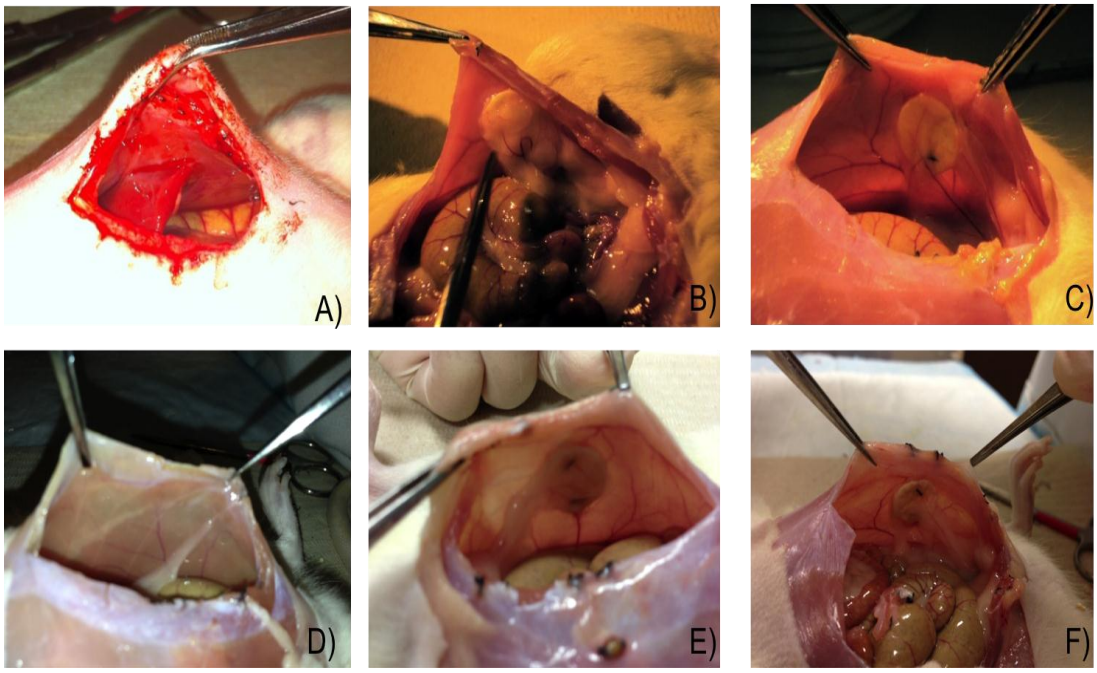

Figure 3.15 Injured sites in the peritoneum for 2 weeks after mesh implantation (A) control, (B) PCL10, (C) PCL10BPLP3, and for 8 weeks after mesh implantation (D) control, (E) PCL10, (F) PCL10BPLP3.

The pictures in Figure 3.15 (A-C) are representative images all three samples at 2 weeks. For the control, the adhesion scores were rated mostly 1 (*), with one sample rated as high as 3 (***). The PCL10 mesh was rated most commonly at 2 (**), indicating moderate adhesion formation for most of the samples. The PCL10BPLP3 had two samples at 2 (**) and one sample observed that had no adhesion formation 0(-).

Based on the acute adhesion formation, it is determined that the PCL10BPLP3 mesh did not form as much adhesion as PCL10 membrane.

The values in Table 3.5 indicate the scores observed for each sample at 8 weeks, signifying chronic adhesion. The pictures in Figure 3.15 (D-F) are representative images for all three samples at 8 weeks. For the control, the adhesion scores were rated equally between 1 (*) or 2 (**). The PCL10 membrane had mostly severe adhesion formations at 3 (***), while the PCL10BPLP3 had over half of the sample yielding slight adhesion presence 1 (*).

Unexpectedly, from the results, it was noted that the control appeared to have less or as much adhesion as the other samples for both time points. It is speculated that this occurred due to that the animal model used in our preliminary *in vivo* studies is not ideal. With the animal model used for this study, it is difficult to keep each procedure consistent. Peritoneal wall wounds created by the surgeon will vary in severity in each animal. Also, the disturbance imposed on the organ will differ in severity. Thus, it is possible that the injury for the control samples was not severe enough to elicit significant adhesion formations. It is also speculated that the PCL10 and PCL10BPLP3 samples mostly had at least a 1 (*) score based on the foreign body reaction to the implanted mesh as well as the sutured sites. In fact, adhesion that was present on the PCL10BPLP3 membrane was mostly accumulated around the suture sites, and not on the membrane surface itself. Since the surface of the PCL10BPLP3 mesh was not entirely smooth, it is also a possibility that adhesion may have occurred due to tissue abrasion by the mesh surface. However, the PCL10BPLP3 contained better adhesion

scores than PCL10 at both time points. This was expected due to the hydrophobic surface property of PCL10 mesh, determined from contact angle studies (Section 3.2.1). Thus, with incorporation of BPLP, the barrier performance of electrospun meshes was improved.

3.3.3 Histological Analysis

Histological analysis was conducted at two time points, 2 weeks and 8 weeks. 6 rats were sacrificed at 2 weeks and 4 rats at 8 weeks. Hematoxylin-eosin (H&E) staining was used on the samples for adhesion analysis. Representative images of histological samples stained with H&E are provided in Figure 3.16, 3.17, and 3.18 at 4x and 10x magnification.

Histological images for all samples in Figure 3.16, 3.17 and 3.18 are indicative of subacute response of the body. The images provide an overall view of the wound/implantation site. During the sub-acute inflammation, initial inflammatory substances accrue along the wound region. These substances include a culmination of macrophages, lymphocytes, and small blood vessels [21]. The control site appears to have a high inflammation, suggesting healing of the wound that was created during operation. PCL10 also appears to have an elevated inflammatory response along the edges of the mesh, indicating adhesion initiation. PCL10BPLP3 has the least amount of inflammation, revealing the effectiveness of using this membrane for anti-adhesion purposes. From water contact angle studies in Section 3.1.4, PCL10 membrane was found to be hydrophobic. Since PCL10 possesses this property, a greater variety of cells with wider cell diameter ranges are attracted to the mesh surface as opposed to the

surface of PCL10BPLP3. The slight cell infiltration that occurred for PCL10BPLP3 membrane is observed along the edges of the mesh, where degradation occurred. Thus, PCL10BPLP3 has less penetration of inflammatory contents than the PCL10 membrane.

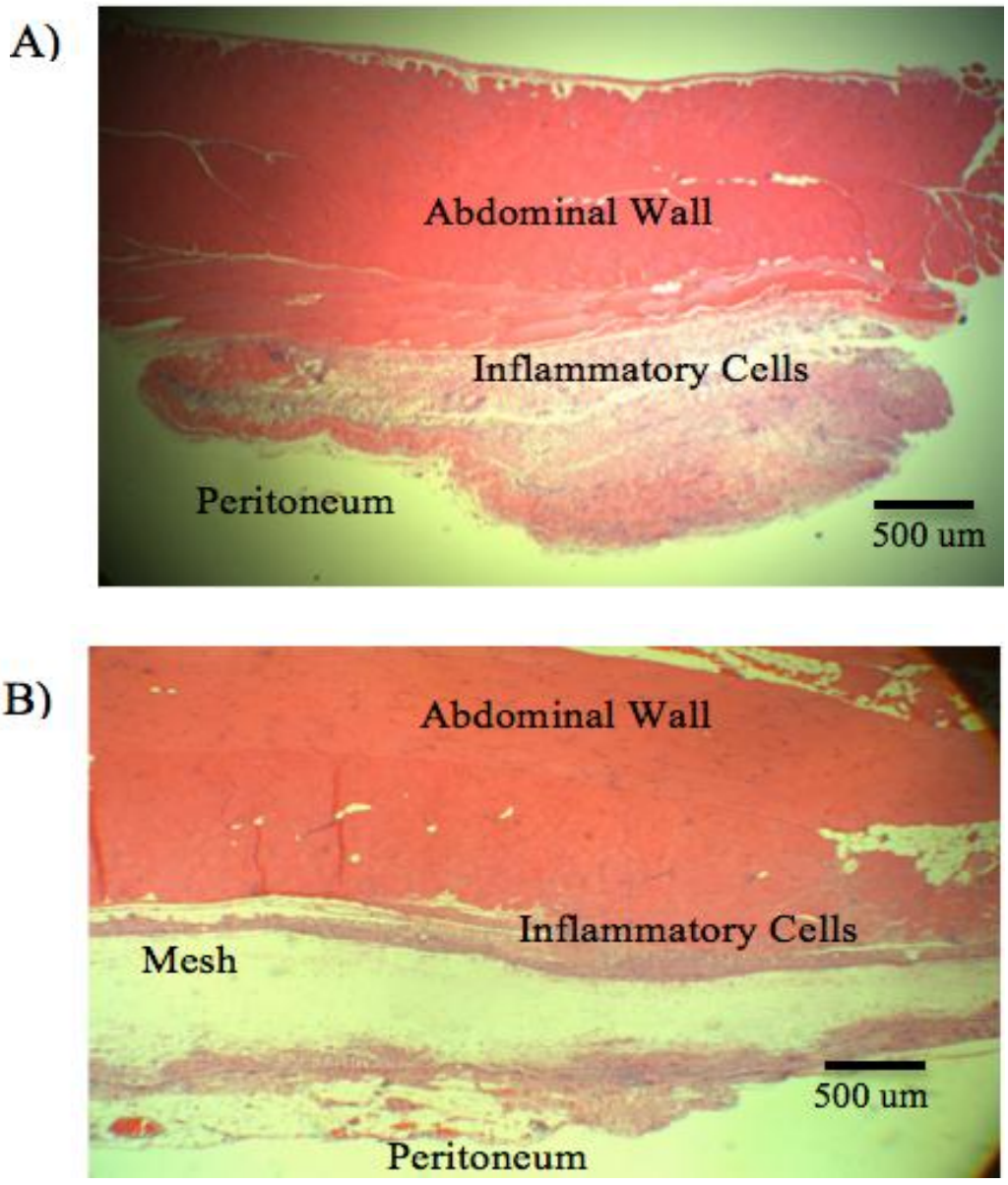

Figure 3.16 Histological staining with hematoxylin-eosin at 4x: (A) Control site, (B) PCL10 at 2 weeks.

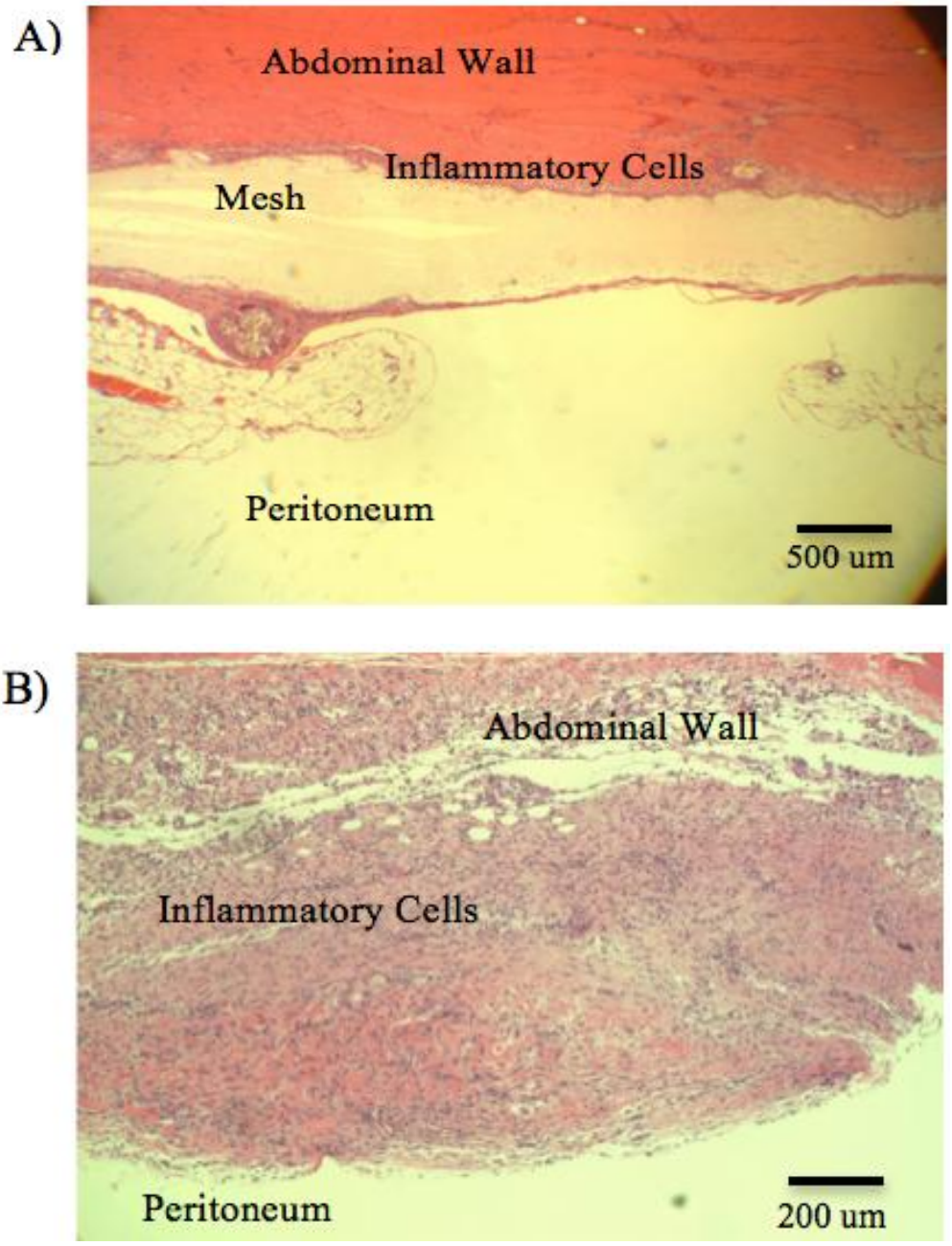

Figure 3.17 Histological staining with hematoxylin-eosin (A) PCL10BPLP3 (4x) and (B) Control site (10x) at 2 weeks.

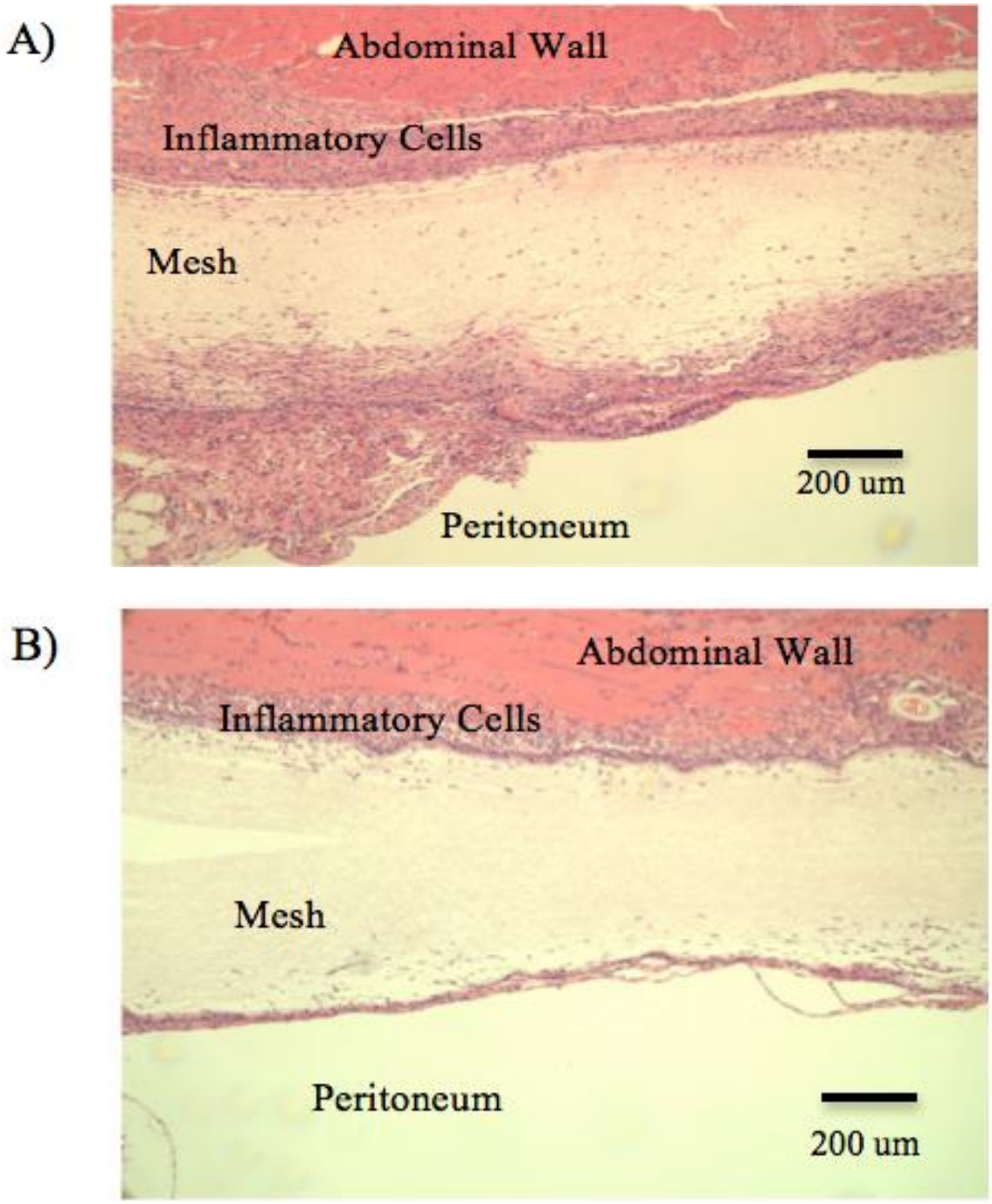

Figure 3.18 Histological staining with hematoxylin-eosin at 10x (A) PCL10 and (B) PCL10BPLP3 for 2 weeks.

The fibrous capsules developed along the samples were measured for thickness. Figure 3.19 indicates the thickness of the fibrous capsules along the exterior (peritoneal) side of the mesh. The fibrous capsule accumulated around the PCL10BPLP3 is drastically thinner at 39± 11.7 μm than the PCL10 samples at 262 ± 105.8 μm and control at 586 ± 369.2 μm. Since the fibrous capsule is thinnest for PCL10BPLP3 mesh, it can be concluded that this membrane has the less potential for adhesion when compared to using PCL10 or using nothing.

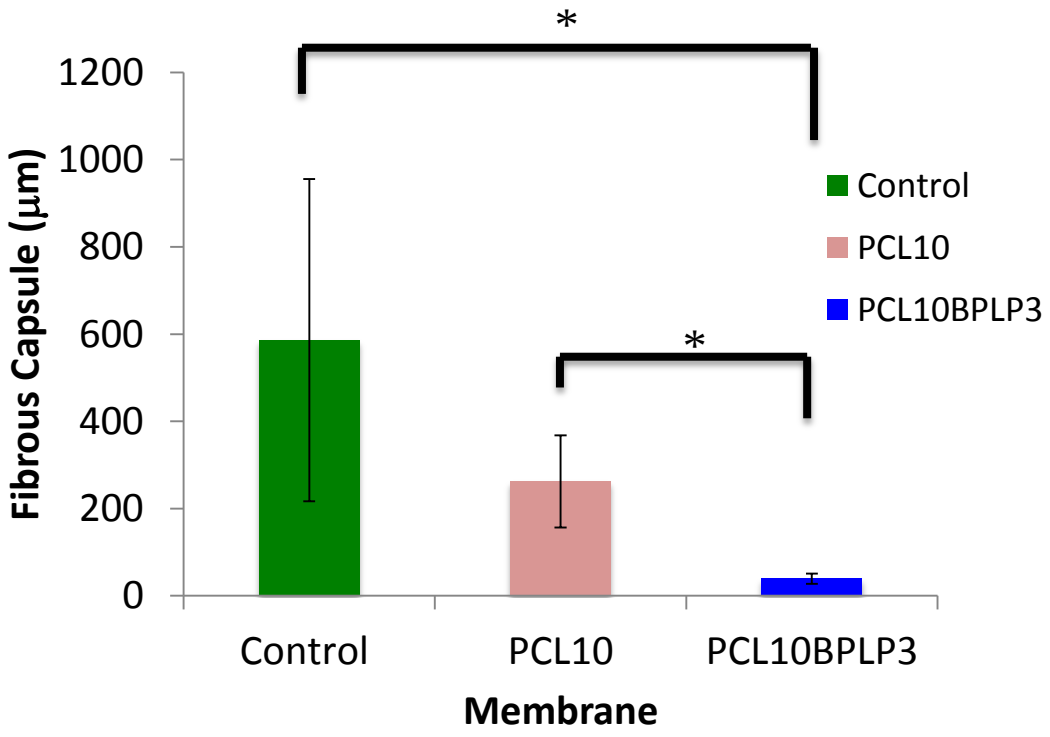

Figure 3.19 Fibrous capsule layer thickness at 2 weeks

3.3.4 In Vivo Degradation

For the *in vivo* degradation study, the samples were weighed after 8 weeks of implantation in the peritoneal cavity and compared with weight before implantation. To

facilitate removal of extraneous tissue/bodily substances from the mesh, the samples were placed in trypsin for 48 hours. After 8 weeks, 107 ± 7.5 % of the weight was remaining for the PCL10 membrane, and 82 ± 11.3% of the weight remained for the PCL10BPLP3 membrane. There is a significant difference between the weight remaining values of each membrane ($P<0.05$), concluding that the PCL10BPLP3 membrane degrades significantly faster *in vivo* than PCL itself. The weight remaining values from the *in vitro* degradation study are consistent with values from the *in vivo* degradation study for both types of membrane. Despite using trypsin to remove any leftover bodily tissue that may have adhered to the membranes, there was still a slight tissue amount or other inflammatory substances that remained on the mesh. This would explain why the weight remaining of PCL10 after implantation was greater than the initial weight. As determined by contact angle studies in Section 3.1.4, PCL10 had a hydrophobic surface property, which would have attracted more inflammatory proteins after trauma had occurred within the peritoneum. One of the main drawbacks in a study conducted by Bolgen and associates, where PCL was used solely as membrane, was the slow degradability in the body [21] . In comparison, PCL10BPLP3 mesh is superior for biodegradability.

CHAPTER 4

CONCLUSIONS AND FUTURE STUDIES

In this study, a novel biodegradable membrane has been fabricated by blending PCL and BPLP in a synergistic combination to prevent post-surgical adhesions. These polymers were used for properties that would contribute to preventing post-surgical adhesion and enhancing membrane degradation. PCL provided quick and easy fabrication, excellent mechanical properties and cytocompatibility to BPLP, while BPLP added hydrophilic surface properties and promoted biodegradability. These polymers were not only successfully blended and electrospun together, but both delivered desirable properties to the membranes. From our *in vivo* results, we found that our fabricated membrane, PCL10BPLP3, had higher anti-adhesion performance and much faster degradation rate than PCL alone. Our results indicate that PCL10BPLP mesh has excellent potential for future clinical studies.

Further studies should be conducted to smoothen the surface of the mesh, to increase degradation rate, to improve the animal model and to include comparisons with commercially available membranes. Additionally, collagenase could be used as an alternative to trypsin for the *in vivo* degradation studies to potentially remove all tissues and proteins remained on the membrane and to avoid any damage to the membrane material. Also, further investigations should be implemented to avoid suture adhesion. Fluorescent properties of BPLP should be investigated for *in vivo* imaging to evaluate

degradation *in vivo* and eliminate the need to re-operate. The animal model should be optimized to maintain consistency of wounds created.

REFERENCES

1. Liakakos, T., et al., *Peritoneal adhesions: etiology, pathophysiology, and clinical significance.* Digestive surgery, 2001. 18(4): p. 260-273.
2. Ray Ms, N.F., et al., *Abdominal Adhesiolysis: Inpatient Care and Expenditures in the United States in 1994.* Journal of the American College of Surgeons, 1998. 186(1): p. 1-9.
3. Menzies, D., *Peritoneal adhesions. Incidence, cause, and prevention.* Surgery annual, 1992. 24: p. 27.
4. DeCherney, A.H. and G.S. diZerega, *Clinical Problem of Intraperitoneal Postsurgical Adhesion Formation Following General Urgery and the Use of Adhesion Prevention Barriers* Surgical Clinics of North America, 1997. 77(3): p. 671-688.
5. James M. Becker, A.F.S., Karen L. Reed, *Abdominal Adhesions*, in *National Institutes of Health*2009, Clearinghouse: Bethesda, MD.
6. Hellebrekers, B.W.J., et al., *Use of fibrinolytic agents in the prevention of postoperative adhesion formation.* Fertility and sterility, 2000. 74(2): p. 203-212.
7. Zong, X., et al., *Prevention of postsurgery-induced abdominal adhesions by electrospun bioabsorbable nanofibrous poly (lactide-co-glycolide)-based membranes.* Annals of surgery, 2004. 240(5): p. 910.

8. Hellebrekers, B., et al., *Effects of five different barrier materials on postsurgical adhesion formation in the rat.* Human Reproduction, 2000. 15(6): p. 1358-1363.

9. Stangel, J., J. Nisbet 2nd, and H. Settles, *Formation and prevention of postoperative abdominal adhesions.* The Journal of reproductive medicine, 1984. 29(3): p. 143.

10. Committee, A.P., *Pathogenesis, consequences and control of peritoneal adhesions in gynecologic surgery.* Fertil Steril, 2008. 90: p. S144-S149.

11. Jenney, C.R. and J.M. Anderson, *Adsorbed serum proteins responsible for surface dependent human macrophage behavior.* Journal of biomedical materials research, 2000. 49(4): p. 435-447.

12. Milligan, D. and A. Raftery, *Observations on the pathogenesis of peritoneal adhesions: a light and electron microscopical study.* British Journal of Surgery, 2005. 61(4): p. 274-280.

13. Wahlgren, M. and T. Arnebrant, *Protein adsorption to solid surfaces.* Trends in biotechnology, 1991. 9(1): p. 201-208.

14. *Fibrin*, in *Encyclopaedia Britannica* 2012, Encyclopaedia Britannica Encyclopaedia Britannica Online.

15. Anderson, J.M., A. Rodriguez, and D.T. Chang, *Foreign body reaction to biomaterials.* Semin Immunol, 2008. 20(2): p. 86-100.

16. Pijlman, B.M., et al., *Prevention of adhesions.* European Journal of Obstetrics & Gynecology and Reproductive Biology, 1994. 53(3): p. 155-163.

17. Lauder, C.I.W., A. Strickland, and G.J. Maddern, *Use of a Modified Chitosan–Dextran Gel to Prevent Peritoneal Adhesions in a Porcine Hemicolectomy Model.* Journal of Surgical Research, 2012. 176(2): p. 448-454.

18. Chang, J.-J., et al., *Electrospun anti-adhesion barrier made of chitosan alginate for reducing peritoneal adhesions.* Carbohydrate Polymers, 2012. 88(4): p. 1304-1312.

19. Tang, C.L., et al., *A randomized controlled trial of 0.5% ferric hyaluronate gel (Intergel) in the prevention of adhesions following abdominal surgery.* Annals of surgery, 2006. 243(4): p. 449.

20. *Gynecare Intergel Recall*. Potential Lawsuit 2003 August 20, 2012 [cited 2012; Available from: http://www.lawyersandsettlements.com/lawsuit/gynecare-intergel.html - .UH79qxib8Vk.

21. Bölgen, N., et al., *In vivo performance of antibiotic embedded electrospun PCL membranes for prevention of abdominal adhesions.* Journal of Biomedical Materials Research Part B: Applied Biomaterials, 2007. 81B(2): p. 530-543.

22. Dizerega, G.S., *Contemporary adhesion prevention.* Fertility and sterility, 1994. 61(2): p. 219.

23. Bakkum, E., J. Trimbos, and T. Trimbos-Kemper, *Postsurgical adhesion formation and prevention–recent developments.* Reprod Med Rev, 1996. 5: p. 1-13.

24. Haynes, R. and J. Lamer, *Adrenocorticotropic Hormone: Adrenocorticol Steroids and Their Synthetic Analogs: inhibitors of Adrenocorticol Steroid*

Biosynthesis. The Pharmacological Basis of Therapeutics, 5th cd., L. S, Cmod, 1985: p. 1,472-1,506.

25. Grosfeld, J.L., et al., *Excessive morbidity resulting from the prevention of intestinal adhesions with steroids and antihistamines.* Journal of pediatric surgery, 1973. 8(2): p. 221-226.

26. Holtz, G., *Current use of ancillary modalities for adhesion prevention.* Fertility and sterility, 1985. 44(2): p. 174.

27. Insel, P., *Analgesic-antipyretics and anitiinflammatory agents; drugs employed in the treatment of rheumatoid arthritis and gout.* Goodman & Gilman's the pharmacological basis of therapeutics. 8th ed., New York, Pergamon Press, Inc, 1991.

28. Li, H., et al., *Synthesis and Biological Evaluation of a Cross-Linked Hyaluronan-Mitomycin C Hydrogel.* Biomacromolecules, 2004. 5(3): p. 895-902.

29. Chuang, Y.C., et al., *A novel technique to apply a Seprafilm (hyaluronate–carboxymethylcellulose) barrier following laparoscopic surgeries.* Fertility and sterility, 2008. 90(5): p. 1959-1963.

30. Yang, D.-J., et al., *Tissue anti-adhesion potential of biodegradable PELA electrospun membranes.* Acta Biomaterialia, 2009. 5(7): p. 2467-2474.

31. Burns, J., et al., *Preclinical evaluation of Seprafilm bioresorbable membrane.* Eur J Surg Suppl, 1997. 577: p. 40-48.

32. De Iaco, P.A., et al., *Efficacy of a hyaluronan derivative gel in postsurgical adhesion prevention in the presence of inadequate hemostasis.* Surgery, 2001. 130(1): p. 60-64.

33. Ward, B.C. and A. Panitch, *Abdominal adhesions: current and novel therapies.* Journal of Surgical Research, 2011. 165(1): p. 91-111.

34. Attard, J.A. and A.R. MacLean, *Adhesive small bowel obstruction: epidemiology, biology and prevention.* Can J Surg, 2007. 50(4): p. 291-300.

35. Lee, M.-W., et al., *A new anti-adhesion film synthesized from polygalacturonic acid with 1-ethyl-3-(3-dimethylaminopropyl)carbodiimide crosslinker.* Biomaterials, 2005. 26(18): p. 3793-3799.

36. Cho, W.J., S.H. Oh, and J.H. Lee, *Alginate film as a novel post-surgical tissue adhesion barrier.* Journal of Biomaterials Science, Polymer Edition, 2010. 21(6-7): p. 701-713.

37. Arnall, D. *Wound Care Products*. 1999 September 9, 1999; Available from: http://jan.ucc.nau.edu/~daa/woundproducts/products.html.

38. Haney, A. and E. Doty, *A barrier composed of chemically cross-linked hyaluronic acid (Incert) reduces postoperative adhesion formation.* Fertility and sterility, 1998. 70(1): p. 145-151.

39. Group., I.T.A.B.S., *Prevention of postsurgical adhesions by Interceed (TC7), an absorbable adhesion barrier: a prospective, randomized multicenter clinical study.* Fertility and sterility, 1989. 51: p. 933-938.

40. Kayaoglu, H.A., et al., *An assessment of the effects of two types of bioresorbable barriers to prevent postoperative intra-abdominal adhesions in rats.* Surgery today, 2005. 35(11): p. 946-950.

41. *Overview: Gynecare Interceed*. 2010; Available from: http://www.pelvichealthsolutions.com/gynecare-interceed.

42. Liakakos, T., et al., *Peritoneal adhesions: etiology, pathophysiology, and clinical significance. Recent advances in prevention and management.* Dig Surg, 2001. 18(4): p. 260-73.

43. Haney, A., et al., *Expanded polytetrafluoroethylene (Gore-Tex Surgical Membrane) is superior to oxidized regenerated cellulose (Interceed TC7+) in preventing adhesions.* Fertility and sterility, 1995. 63(5): p. 1021.

44. Farquhar, C., et al., *Barrier agents for preventing adhesions after surgery for subfertility.* The Cochrane Library, 2008.

45. Matsuda, S., et al., *Evaluation of the antiadhesion potential of UV cross-linked gelatin films in a rat abdominal model.* Biomaterials, 2002. 23(14): p. 2901-2908.

46. Buckenmaier, C.C., 3rd, et al., *Comparison of antiadhesive treatments using an objective rat model.* Am Surg, 1999. 65(3): p. 274-82.

47. Nam, J., et al., *Modulation of embryonic mesenchymal progenitor cell differentiation via control over pure mechanical modulus in electrospun nanofibers.* Acta biomaterialia, 2011. 7(4): p. 1516-1524.

48. Hsieh, S.R., et al., *Preparation and non-invasive in-vivo imaging of anti-adhesion barriers with fluorescent polymeric marks.* J Fluoresc, 2009. 19(4): p. 733-40.

49. Wilson, C.J., et al., *Mediation of biomaterial-cell interactions by adsorbed proteins: a review.* Tissue engineering, 2005. 11(1-2): p. 1-18.

50. Nygren, H., *Initial reactions of whole blood with hydrophilic and hydrophobic titanium surfaces.* Colloids and surfaces B: Biointerfaces, 1996. 6(4): p. 329-333.

51. Goldberg, E.P., J.W. Sheets, and M.B. Habal, *Peritoneal adhesions: prevention with the use of hydrophilic polymer coatings.* Archives of Surgery, 1980. 115(6): p. 776.

52. Lee, J.H., et al., *Tissue anti-adhesion potential of ibuprofen-loaded PLLA–PEG diblock copolymer films.* Biomaterials, 2005. 26(6): p. 671-678.

53. Dietschweiler, C., *Protein adsorption at solid surfaces*, M. Sander, Editor, Swiss Federal Institute of Technology: Zurich, Switzerland.

54. Kleijn, J. and W. Norde, *The adsorption of proteins from aqueous solution on solid surfaces.* Heterogeneous Chemistry Reviews, 1995.

55. Roach, P., D. Farrar, and C.C. Perry, *Interpretation of protein adsorption: surface-induced conformational changes.* Journal of the American Chemical Society, 2005. 127(22): p. 8168-8173.

56. Haynes, C.A. and W. Norde, *Globular proteins at solid/liquid interfaces.* Colloids and Surfaces B: Biointerfaces, 1994. 2(6): p. 517-566.

57. Attard, J.A.P. and A.R. MacLean, *Adhesive small bowel obstruction: epidemiology, biology and prevention.* Canadian Journal of Surgery, 2007. 50(4): p. 291.

58. Diamond, M.P., et al., *Adhesion reformation: reduction by the use of Interceed (TC7) plus heparin.* Journal of gynecologic surgery, 1991. 7(1): p. 1-6.

59. Becker, J.M., et al., *Prevention of postoperative abdominal adhesions by a sodium hyaluronate-based bioresorbable membrane: a prospective, randomized, double-blind multicenter study.* Journal of the American College of surgeons, 1996. 183(4): p. 297.

60. Murugan Ramalingam, Z.H., Seeram Ramakrishna, Hisatoshi Kobayashi, Youssef Haikel, *Integrated Biomaterials in Tissue Engineering*. 1st ed. Vol. 1. 2012, Hoboken, New Jersey and Salem, Massachusetts: John Wiley & Sons, Inc. and Scrivener Publishing LLC. 302.

61. Smith, L. and P. Ma, *Nano-fibrous scaffolds for tissue engineering.* Colloids and surfaces B: biointerfaces, 2004. 39(3): p. 125-131.

62. Yang, J., et al., *Development of aliphatic biodegradable photoluminescent polymers.* Proc Natl Acad Sci U S A, 2009. 106(25): p. 10086-91.

63. Peña, J., et al., *Long term degradation of poly (< i> ε</i>-caprolactone) films in biologically related fluids.* Polymer Degradation and Stability, 2006. 91(7): p. 1424-1432.

64. Koski, A., K. Yim, and S. Shivkumar, *Effect of molecular weight on fibrous PVA produced by electrospinning.* Materials Letters, 2004. 58(3): p. 493-497.

65. Subbiah, T., et al., *Electrospinning of nanofibers.* Journal of Applied Polymer Science, 2005. 96(2): p. 557-569.

66. Reneker, D.H. and I. Chun, *Nanometre diameter fibres of polymer, produced by electrospinning.* Nanotechnology, 1999. 7(3): p. 216.

67. Khil, M.S., et al., *Electrospun nanofibrous polyurethane membrane as wound dressing.* Journal of Biomedical Materials Research Part B: Applied Biomaterials, 2003. 67(2): p. 675-679.

68. Formhals, A., *Process and apparatus fob pbepabing*, 1934, Google Patents.

69. Wannatong, L., A. Sirivat, and P. Supaphol, *Effects of solvents on electrospun polymeric fibers: preliminary study on polystyrene.* Polymer International, 2004. 53(11): p. 1851-1859.

70. Doshi, J. and D.H. Reneker, *Electrospinning process and applications of electrospun fibers.* Journal of electrostatics, 1995. 35(2): p. 151-160.

71. Agarwal, S., J.H. Wendorff, and A. Greiner, *Use of electrospinning technique for biomedical applications.* Polymer, 2008. 49(26): p. 5603-5621.

72. Li, W.J., et al., *Electrospun nanofibrous structure: a novel scaffold for tissue engineering.* Journal of biomedical materials research, 2002. 60(4): p. 613-621.

73. You, Y., et al., *In vitro degradation behavior of electrospun polyglycolide, polylactide, and poly(lactide-co-glycolide).* Journal of Applied Polymer Science, 2005. 95(2): p. 193-200.

74. Guertin, D.A., *Cell size control.* Encyclopedia of Life Sciences, 2005: p. 1-10.

75. Bölgen, N., et al., *In vitro and in vivo degradation of non-woven materials made of poly (ε-caprolactone) nanofibers prepared by electrospinning under different conditions.* Journal of Biomaterials Science, Polymer Edition, 2005. 16(12): p. 1537-1555.

76. Onderdonk, A.B., et al., *Experimental intra-abdominal abscesses in rats: quantitative bacteriology of infected animals.* Infection and immunity, 1974. 10(6): p. 1256-1259.

BIOLOGICAL INFORMATION

Pouriska Kivanany was born and raised in Dallas, TX. She attended Plano East Senior High School and graduated from the IB program in 2008. It was during high school that Pouriska conducted summer research at UTD and developed in interest in bioengineering. After exploring many bioengineering programs at various universities, she decided to enroll in the joint 5 year Bachelor's to Master's Bioengineering Program at the University of Texas at Arlington and University of Texas at Southwestern Medical Center Fall 2008. She took classes from different engineering and biological fields, but after taking Biomaterials and Blood Compatibility in Fall 2011, she developed a strong interest in biomaterial research. She began working in Dr. Jian Yang's Biomaterials and Tissue Engineering Laboratory, working on BPLP polymers. Pouriska earned her Bachelor's of Science in Biology and Master's of Science in Biomedical Engineering in December 2012. She looks forward to beginning her doctoral studies Fall 2013 and advancing her research further in biomedical engineering.